MULTILAYERED EQUILIBRIA IN A DENSITY FUNCTIONAL MODEL OF COPOLYMER-SOLVENT MIXTURES

KARL GLASNER

Abstract. This paper considers a free energy functional and corresponding free boundary problem for multilayered structures which arise from a mixture of a block copolymer and a weak solvent. The free boundary problem is formally derived from the limit of large solvent/polymer segregation and intermediate segregation between monomer species. A change of variables based on Legendre transforms of the effective bulk energy is used to explicitly construct a family of equilibrium solutions. The second variation of the effective free energy of these solutions is shown to be positive. This result is used to show more generally that equilibria are local minimizers of the free energy.

Block copolymers are molecularly bonded mixtures of two distinct polymer species. They may exhibit *microphase segregation*, wherein small domains of heterogeneous composition form. The size of these domains is limited by the energy penalty of polymer stretching. In contrast, a mixture of copolymer and another phase (here a weak solvent) may undergo *macrophase segregation*, wherein there is no such limit to the sizes of polymer and solvent domains. The combined effect of both types of phase segregation leads to a wide variety of morphologies [1–6].

Density functional models of inhomogeneous polymer systems now have a long history [7–9]. These involve a free energy which depends explicitly on volume fractions of the individual system components, and generally take the form of Cahn-Hilliard [10] energies combined with nonlocal terms which penalize polymer stretching. A model for mixtures of diblock copolymers and another partially miscible phase was first considered by Ohta and Ito [3] and carefully re-derived by Choksi and Ren [11]. Subsequently a related sharp interface model was proposed by van Gennip and Peletier [12] who study global energy minimizers.

Both experimental observations [13, 14] and numerical simulations of density functional models [3,6] reveal that polymer/solvent systems which have both micro- and macrophase segregation lead to layered domain patterns composed of alternating block copolymer composition, surrounded by solvent. The simplest of these structures are monolayers, consisting of two adjacent monomer-rich domains, and bilayers (c.f. figure 1), consisting of three polymer-rich domains. The latter are the synthetic analog of biological lipid bilayers; a variety of mathematical models for these type of structures have been studied in recent years [15–18]. Multilayered structures play a significant role in higher dimensions: they are the basis for membrane-like interfaces which are widely observed to fold and form closed surfaces (e.g. "multilamellar vesicles" [13]).

This work is a starting point to analyze morphology of multilayered block copolymer structures. We study the most basic problem, which is to determine the cross-sectional profile of a multilayered interface; this amounts to an investigation of one-dimensional equilibria and their stability. This paper does this in several steps:

- The formulation of the static (3-4) and dynamic (6-7) problems arising from a density functional is reviewed in section 1. The static problem represents the Euler-Lagrange system for an unbounded system with a specified far-field chemical potential, whereas the dynamic problem is a coupled system of parabolic equations.
- One dimensional free boundary problems which describe both polymer/polymer and polymer/solvent interfaces (equations (F1-F3) and (F1'-F3')) are derived formally in the

limits of small domain interface width in section 2. This problem serves as a basis for a rigorous study of equilibria and their stability. We note a similar problem has been analyzed by Fife and Hilhorst [19] in the simpler solvent-free case. We also propose a reduced free energy functional and show that it serves as a Lyapunov function for the dynamic free boundary problem.

- Multilayered equilibria are shown to exist over a range of parameters in section 3. These are constructed explicitly by a change of variables that allows the use of dynamical systems arguments.
- Stability of equilibria (in the one-dimensional sense) is considered in section 4. This is done (section 4.1) by reducing the question of positivity of the second variation of the free energy to a finite dimensional linear problem, whose associated quadratic form is shown to be positive.
- Equilibria are shown to be local minimizers of the reduced energy in section 4.2. This involves using the second variation in conjunction with straightforward estimates on higher order contributions.

1. Model formulation

Density functional models of polymer systems describe the free energy as a function of composition variables ϕ_i, $i = 1, 2, 3, \ldots$. For a system with physical domain Ω (here $\Omega = \mathbb{R}$), these have a generic structure

$$\int_\Omega \left(W(\phi_1, \phi_2, \ldots) + \sum_{i,j} \varepsilon_{ij} \nabla\phi_i \cdot \nabla\phi_j \right) dx + \sum_{i,j} \alpha_{ij} I_{ij}$$

The first term is a bulk energy potential W with minima corresponding to bulk phases (where only one ϕ_j is nonzero), which by itself promotes phase separation. The gradient terms typically penalize sharp interfaces and promote phase mixing. The final term is a nonlocal energy

$$I_{ij} = \int_\Omega \int_\Omega G(x, x')(\phi_i(x) - \overline{\phi}_i)(\phi_j(x') - \overline{\phi}_j)\, dx\, dx'.$$

where G is a nonlocal interaction kernel (taken to be the Laplacian Green's function here) and $\overline{\phi}_i$ is the average volume fraction of species i.

The present system under consideration has three species A, B, C where A and B comprise components of a copolymer and C is a distinct molecular species. A typical assumption is incompressibility

$$\phi_A + \phi_B + \phi_C = 1,$$

which allows for one compositional variable to be eliminated. Ohta and Nonomura [20] reformulated this model by diagonalizing the nonlocal interaction matrix by setting

$$\Phi = (1 - f)\phi_A - f\phi_B, \quad \Psi = f\phi_A + (1 - f)\phi_B, \tag{1}$$

where f is the fraction of A-monomer compared to the total copolymer volume. Note the compositional variable Ψ measures the presence of polymer, whereas Φ represents the relative preponderance of each monomer. The resulting free energy can be written

$$E = \int_\Omega W(\Phi, \Psi) + \frac{\epsilon_{11}^2}{2}|\nabla\Phi|^2 + \epsilon_{12}(\nabla\Phi \cdot \nabla\Psi) + \frac{\epsilon_{22}^2}{2}|\nabla\Psi|^2 dx + \frac{\alpha}{2}\int_\Omega \int_\Omega G(x, x')\Phi(x)\Phi(x')\, dx\, dx'. \tag{2}$$

The potential $W(\Phi, \Psi)$ has minima at $(\Phi, \Psi) = (0, 0)$, corresponding to pure solvent, and $(\Phi, \Psi) = (1 - f, f)$ and $(-f, 1 - f)$ corresponding to pure A or B monomer, respectively.

Figure (1) illustrates the type of configurations we shall study, which turn out to be approximated by local minimizers of a reduced energy. The figure shows a bilayer equilibrium, in which

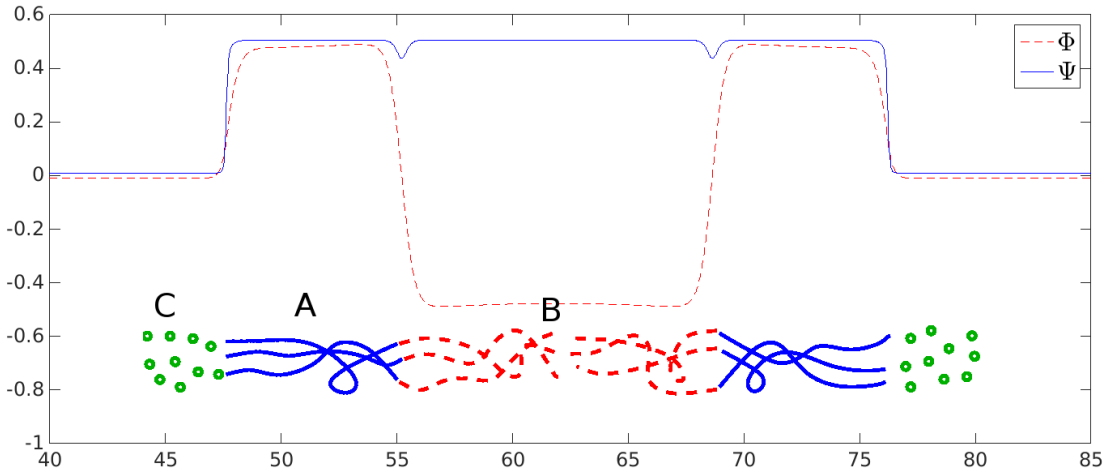

FIGURE 1. A numerically computed equilibrium bilayer solution with an illustration of the corresponding molecular configuration. The solvent phase (green/circles) occupies the domains to the far left and far right. The A-monomer phase (blue/solid) occupies the right and left inner domains. The B-monomer phase (red/dashed) occupies the middle domain.

the B-rich subdomain is surrounded by two A-rich subdomains. In general, we will show that equilibria can be constructed to have any number of subdomains larger than one.

1.1. **Formulation for equilibria and dynamics.** In finite domains, global energy minimizers are typically studied in conjunction with constraints which preserve total volume of each polymer species (e.g. [12]). In contrast, our interest is an *infinite* domain, where volume-constrained energy minimizers do not exist (see section 5.1). The formulation used here supposes that localized equilibria are in thermodynamic equilibrium with their environment. This means that rather than prescribing the polymer volume, the associated chemical potential $\mu_\Psi = \delta E/\delta\Psi$ is prescribed at infinity instead. In the present case, this means that equilibrium solutions satisfy the Euler-Lagrange system

$$(-\epsilon_{11}^2\Phi_{xx} - \epsilon_{12}\Psi_{xx} + W_\Phi)_{xx} = \alpha\Phi \tag{3}$$

$$-\epsilon_{22}^2\Psi_{xx} - \epsilon_{12}\Phi_{xx} + W_\Psi = \mu_\Psi. \tag{4}$$

The relevant far-field conditions are chosen by supposing that layered copolymer domains occupy a spatially localized region and that only a small uniform concentration of polymer is present far away. This is encoded by the conditions

$$\lim_{x\to\pm\infty}\Phi = 0, \quad \lim_{x\to\pm\infty}\Psi = \Psi_\infty, \quad W_\Psi(0,\Psi_\infty) = \mu_\Psi. \tag{5}$$

The last expression means that specifying the far field polymer concentration Ψ_∞ is equivalent to choosing μ_Ψ.

We will also briefly consider a time dependent problem which leads to equilibrium. Dynamical models typically arise from diffusion driven by gradients of the generalized chemical potentials $\delta E/\delta\Phi$ and $\delta E/\delta\Psi$; this leads to

$$M_\Phi^{-1}\Phi_t = (-\epsilon_{11}^2\Phi_{xx} - \epsilon_{12}\Psi_{xx} + W_\Phi)_{xx} - \alpha\Phi \tag{6}$$

$$M_\Psi^{-1}\Psi_t = (-\epsilon_{22}^2\Psi_{xx} - \epsilon_{12}\Phi_{xx} + W_\Psi)_{xx}. \tag{7}$$

where M_Φ, M_Ψ are mobility coefficients. Consideration of the dynamics is limited to the case where polymer/solvent phase segregation is rapid compared to segregation of polymers. With a suitable choice of timescale, we can make $M_\Phi = 1$ and $M_\Psi \gg 1$. The latter results in $-\epsilon_{22}^2\Psi_{xx} - \epsilon_{12}\Phi_{xx} + W_\Psi = \mu_\Psi$ at leading order.

The systems (6-7) or (3-4) represent a coupling of the Ohta-Kawasaki [8] equation describing microscopic phase segregation, and the Cahn-Hillard equation [10] describing macroscopic phase segregation.

1.2. **Properties of the bulk potential.** For purposes of this paper, $W : \mathbb{R}^2 \to \mathbb{R}$ is in C^2 with bounded derivatives. The three minima of W will be assumed to be equal, and for convenience set to zero. Note this can always be achieved by addition of a linear function of Φ and Ψ, which does not alter the form of the governing equations (6-7). The other technical properties which are needed are listed below.

(P1) For each μ_Ψ in the interval $0 < \mu_\Psi < \mu_\Psi^{max} \equiv W_\Psi(0, \Psi^{max})$, there exist unique values $\Phi_{t+} > 0$, $\Phi_{t-} < 0$, $\Psi_{a\pm}$, $\Psi_{b\pm}$ (defined so that $\Psi_{a\pm} < \Psi_{b\pm}$), so that the following relations hold:

$$\frac{W(\Phi_{t\pm}, \Psi_{a\pm}) - W(\Phi_{t\pm}, \Psi_{b\pm})}{\Psi_{a\pm} - \Psi_{b\pm}} = \mu_\Psi, \quad W_\Psi(\Phi_{t\pm}, \Psi_{a\pm}) = \mu_\Psi = W_\Psi(\Phi_{t\pm}, \Psi_{b\pm}).$$

The motivation for this statement is the internal layer problem (12), whose solution is a diffuse interface for Ψ connecting asymptotic values Ψ_{a+} and Ψ_{b+} (or Ψ_{a-} and Ψ_{b-}), and simultaneously selects the value $\Phi \sim \Phi_{t\pm}$ within the layer (see figure 4).

(P2) There are continuously differentiable functions $\Psi_{1,2} : [-f, 1-f] \times [0, \mu_\Psi^{max}] \to \mathbb{R}$ which satisfy the nullcline relations

$$W_\Psi(\Phi, \Psi_{1,2}(\Phi; \mu_\Psi)) = \mu_\Psi, \tag{8}$$

where

$$\max_{\Phi_{t-} < \Phi < \Phi_{t+}} \Psi_1(\Phi; \mu_\Psi) \leq \min_{-f < \Phi < 1-f} \Psi_2(\Phi; \mu_\Psi).$$

We suppose that Ψ_1 and Ψ_2 are the only functions satisfying (8). As long as μ_Ψ is small, the curve $\Psi = \Psi_1(\Phi; \mu_\Psi)$ passes near the minimum of W at the origin, whereas $\Psi = \Psi_2(\Phi; \mu_\Psi)$ passes near the other two minima (see figure 5).

(P3) It will be useful to define an effective potential by

$$\tilde{W}(\Phi) = \begin{cases} W(\Phi, \Psi_1(\Phi; \mu_\Psi)) - \mu_\Psi \Psi_1(\Phi; \mu_\Psi), & \Phi_{t-} \leq \Phi \leq \Phi_{t+} \\ W(\Phi, \Psi_2(\Phi; \mu_\Psi)) - \mu_\Psi \Psi_2(\Phi; \mu_\Psi), & \Phi > \Phi_{t+} \text{ or } \Phi < \Phi_{t-}, \end{cases} \tag{9}$$

Using property P1, it follows that $\tilde{W}$ is continuous at $\Phi_{t\pm}$. In addition, it is easily checked that $\tilde{W}'(\Phi) = W_\Phi(\Phi, \Psi_{1,2}(\Phi; \mu_\Psi))$. It is supposed that $\tilde{W}$ is convex in the three intervals delineated by Φ_{t-} and Φ_{t+} (see figure 3). Analogous to property P1, if $0 < \mu_\Psi < \mu_\Psi^{max}$ it is supposed that there exists constants $\Phi_{a\pm}, \Phi_{b\pm}, \Phi_\pm, \mu_{\Phi\pm}$ and μ_Φ so that

$$\Phi_{b-} < \Phi_{t-} < \Phi_{a\pm} < \Phi_{t+} < \Phi_{b+}, \quad \Phi_- < \Phi_{t-} < \Phi_{t+} < \Phi_+,$$

and the following hold:

$$\frac{\tilde{W}(\Phi_{b\pm}) - \tilde{W}(\Phi_{a\pm})}{\Phi_{b\pm} - \Phi_{a\pm}} = \mu_{\Phi\pm}, \quad \tilde{W}'(\Phi_{a\pm}) = \mu_{\Phi\pm} = \tilde{W}'(\Phi_{b\pm}), \tag{10}$$

$$\frac{\tilde{W}(\Phi_+) - \tilde{W}(\Phi_-)}{\Phi_+ - \Phi_-} = \mu_\Phi, \quad \tilde{W}'(\Phi_+) = \mu_\Phi = \tilde{W}'(\Phi_-). \tag{11}$$

These conditions will be used for the internal layer problems in equations (14) and (16).

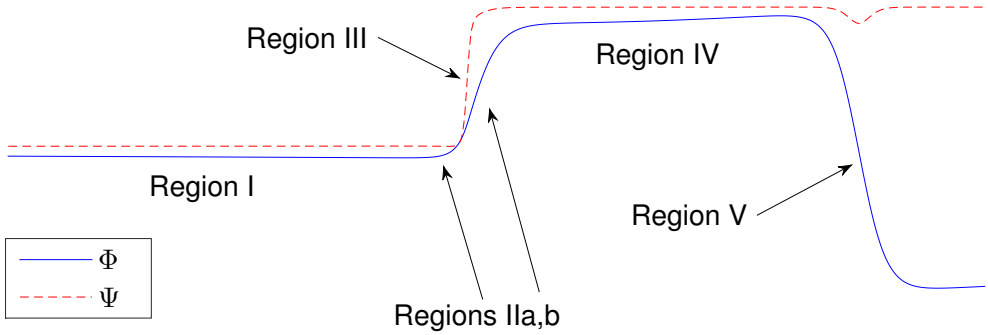

FIGURE 2. Regions for matched asymptotic expansions. Region III is a transition layer inside region II.

Properties P1 and P3 are "common tangent" relations, which arise as a result of local thermodynamic equilibrium of a material interface. Their relation to the Cahn-Hilliard interfaces studied in this paper is recalled in the appendix. We remark that the upper bound on μ_Ψ is not a mere technicality; dynamical behavior which does not lead to equilibrium can ensue if this parameter is too large (see fig. 8).

It is not difficult to construct a polynomial-type function which satisfies these requirements. Illustrations and simulations which appear in this paper employ the potential

$$W(\Phi,\Psi) = \Psi^2(\Psi_m-\Psi)^2+(\Psi_m-\Psi)^2\Phi^2+\frac{1}{2}\Psi^2(\Phi+f)^2(\Phi+f-1)^2, \quad \Psi_m \equiv (2f-1)(\Phi+f)+1-f.$$

2. FREE BOUNDARY REDUCTION FOR STRONG POLYMER-SOLVENT SEGREGATION

Here we formally derive a free boundary problem for the location of internal layers which constitute a multilayered structure. The parameter ϵ_{11} controls the amount of phase separation between A and B monomers, whereas ϵ_{22} controls phase separation between polymer and solvent. The physically typical case is where the latter is a stronger effect; this suggests considering the limiting case

$$\epsilon_{22} \ll \epsilon_{11} \ll 1.$$

In addition, it is supposed that the $\epsilon_{12} \sim \epsilon_{22}^2$ (note this is a mathematical necessity: if ϵ_{12} is too large, the gradient terms in the functional (2) may not be coercive in H^1, and the corresponding variational problems could be ill-posed).

We remark that the parameter α is considered $O(1)$. This is in stark contrast to the more common scaling $\alpha = O(\epsilon_{11})$ chosen for the sharp interface limit of the uncoupled Ohta-Kawasaki equation (equation (6) with the dependency on Ψ suppressed) , which has been considered by Nishiura and Ohnishi [21] in deriving a free boundary evolution, as well as in the Γ-convergence results of Ren and Wei [22]. If we replace α with $\epsilon_{11}\alpha$ in our problem, multilayer domain sizes would scale as $\epsilon_{11}^{-1/2}$.

The limiting problem for small ϵ_{11} can be obtained by a straightforward application of matched asymptotic expansions. The details are similar to those found throughout the literature on diffuse interfaces (e.g. [21, 23, 24]). The regions for the expansion are shown in figure 2. There are two types of internal layers, associated with edge interfaces and interior interfaces between monomer domains (region V). The former type is actually a double layer: there is a rapid transition layer in Ψ (region III) residing within the Φ transition layer (regions IIa and IIb). The regions delineated

by internal layers are of two types: interior domains (region IV), which may be numerous, and two unbounded exterior domains (region I). The non-constant solution in region I describes the extension of polymer chains into the solvent. To avoid a surplus of notation, subscripts associated with asymptotic expansions are omitted until subdominant terms are required in section (2.3).

2.1. **Internal layer solutions.** We first consider the finest internal layers in region III. Supposing this transition layer is located where $x \approx x_j$. Using the stretched variable $z = (x - x_j)/\epsilon_{22}$ the leading order equations for either (3-4) or (6-7) are

$$\Phi_{zzzz} = 0, \quad -\Psi_{zz} - \frac{\epsilon_{12}}{\epsilon_{22}^2}\Phi_{zz} + W_\Psi(\Phi, \Psi) \equiv \mu_\Psi. \tag{12}$$

The second equation arises in the dynamic case from the assumption that $M_\Psi \gg 1$. Asymptotic matching at leading order implies that $\Phi(z) \sim C$ as $z \to \pm\infty$, where C is a constant. It follows that $\Phi(z)$ is identically constant.

The interface problem (12) is essentially the same as for the classical Cahn-Hilliard equation, and it is understood to have a unique solution (up to translation) which simultaneously yields values for $\Psi(z = \pm\infty)$ and μ_Ψ (see [23] and references therein). These quantities are related by the first property of W, so that $\Phi(z) \equiv \Phi_{t+}$ or Φ_{t-}, and

$$\lim_{z\to-\infty} \Psi(z) = \Psi_{a\pm}, \quad \lim_{z\to\infty} \Psi(z) = \Psi_{b\pm}.$$

This is the same as the usual common tangent relation (c.f. [23]), however in our case, μ_Ψ is fixed and $\Phi_{t\pm}$ is selected.

Region II has two parts divided by region III: IIa is adjacent to region I and IIb is adjacent to region IV. In terms of the stretched variable $y = x/\epsilon_{11}$, the leading order equations are

$$\mu \equiv -\Phi_{yy} + W_\Phi(\Phi, \Psi), \quad W_\Psi(\Phi, \Psi) = \mu_\Psi, \quad \mu_{yy} = 0. \tag{13}$$

The second equation in (13) is simply the nullcline relation (8). By construction, region IIa refers to smaller values of Ψ, therefore $\Psi = \Psi_1(\Phi; \mu_\Psi)$ in this region. Similarly, $\Psi = \Psi_2(\Phi; \mu_\Psi)$ in region IIb. The third equation implies (again by leading order matching) that $\mu(y)$ is equal to a constant.

Since the effective potential (9) was defined to be continuous and so that $\tilde{W}'(\Phi) = W_\Phi(\Phi, \Psi_{1,2}(\Phi; \mu_\Psi))$, the problems for regions IIa and IIb can be combined into a single integrable equation

$$-\Phi_{yy} + \tilde{W}'(\Phi) = \mu. \tag{14}$$

Using property P3, the constant $\mu = \mu_{\Phi\pm}$ and the far field behavior is (see figure 4)

$$\lim_{y\to-\infty} \Phi = \Phi_{a\pm}, \quad \lim_{y\to\infty} \Phi = \Phi_{b\pm}, \tag{15}$$

where the choice of signs depends on the sign of Φ in region IV. The phase-plane trajectories $(\Phi(x), \Psi(x))$ of the internal layer solutions in regions II and III are sketched in figure 5, along with the contours of the potential.

Finally, region V uses the same stretched coordinate as region II, and the leading order solution satisfies

$$-\Phi_{yy} + W_\Phi(\Phi, \Psi_2(\Phi, \mu_\Psi)) = \mu, \quad \mu_{yy} = 0, \tag{16}$$

As above, leading order matching implies that $\mu(y)$ must be a constant. Furthermore, equation (16) is the same as $-\Phi_{yy} + \tilde{\tilde{W}}_\Phi = \mu$, where the modified effective potential is $\tilde{\tilde{W}} \equiv W(\Phi, \Psi_2(\Phi, \mu_\Psi)) - \mu_\Psi \Psi_2(\Phi, \mu_\Psi)$, which coincides with $\tilde{W}$ when $\Phi > \Phi_{t+}$ or $\Phi < \Phi_{t-}$. Property P3 then yields

$$\lim_{y\to\pm\infty} \Phi(y) = \Phi_\pm \text{ or } \Phi_\mp, \quad W_\Phi(\Phi_\pm, \Psi_2(\Phi_\pm, \mu_\Psi)) = \tilde{W}'(\Phi_\pm) = \mu = \mu_\Phi, \tag{17}$$

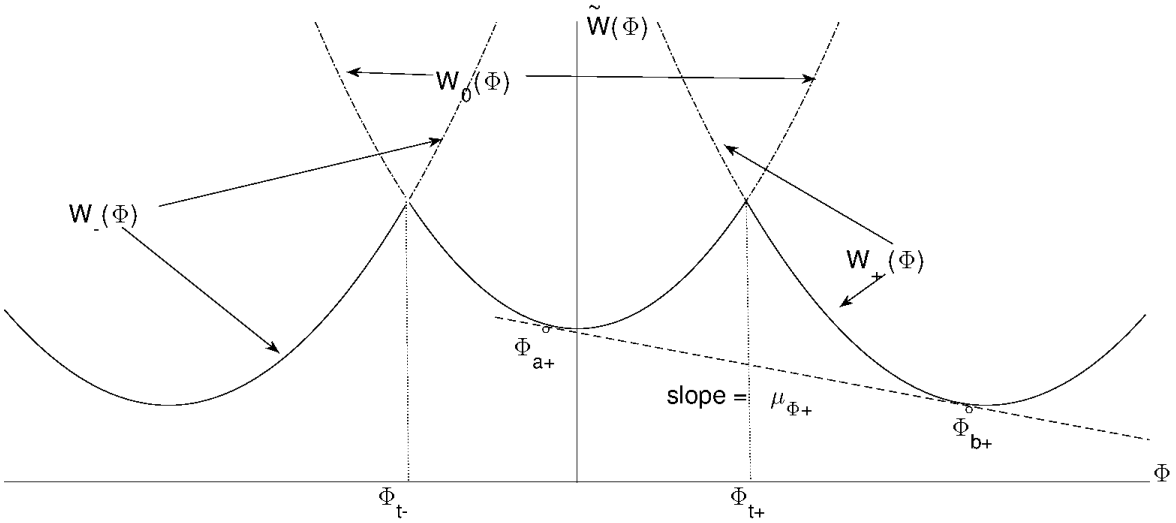

FIGURE 3. The effective potential $\tilde{W}$ (solid) and the corresponding common tangent construction (dotted) for the solution in region II. The convex extensions $W_{+,-,0}$ (dash-dot) are used for analytic convenience later on.

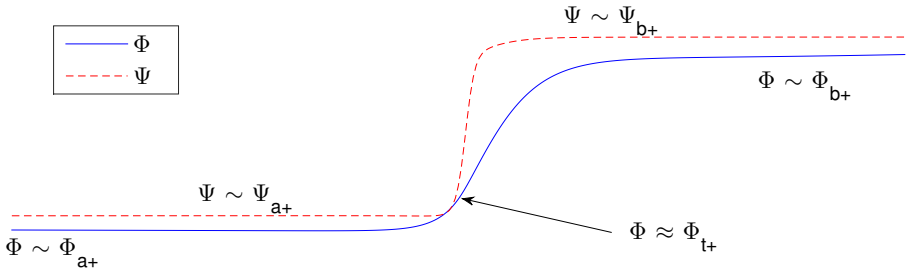

FIGURE 4. Structure of the double internal layer (regions II and III), showing the limiting values $\Phi_{a,b+}$ and $\Psi_{a,b+}$ as the layer is approached from the left or right, as well as the value $\Phi \sim \Phi_t$ in region III.

where the choice of $\pm$ and $\mp$ alternates from one interior interface to the next.

2.2. **Bulk region solutions.** Regions I and IV have potentially dynamic leading order solutions. These satisfy a parabolic nonlinear equation

$$\Phi_t = [W_\Phi(\Phi, \Psi_{1,2}(\Phi, \mu_\Psi))]_{xx} - \alpha\Phi.$$

In terms of the effective potential, this equation reads $\Phi_t = \tilde{W}'(\Phi)_{xx} - \alpha\Phi$. This equation is supplemented by Dirichlet-type boundary conditions provided at each interface by (15) and (17), well as the far-field conditions $\Phi(\pm\infty) = 0$.

2.3. **Motion of interfaces.** We have not yet determined how the motion or location of the internal layers is specified, which require expansions in the small parameter ϵ_{11}. For an internal layer (either region II or V-type) located at $x_j(t)$, we consider the situation where the velocity $dx_j/dt = O(1)$. This reflects the timescale where balance with leading order derivatives of

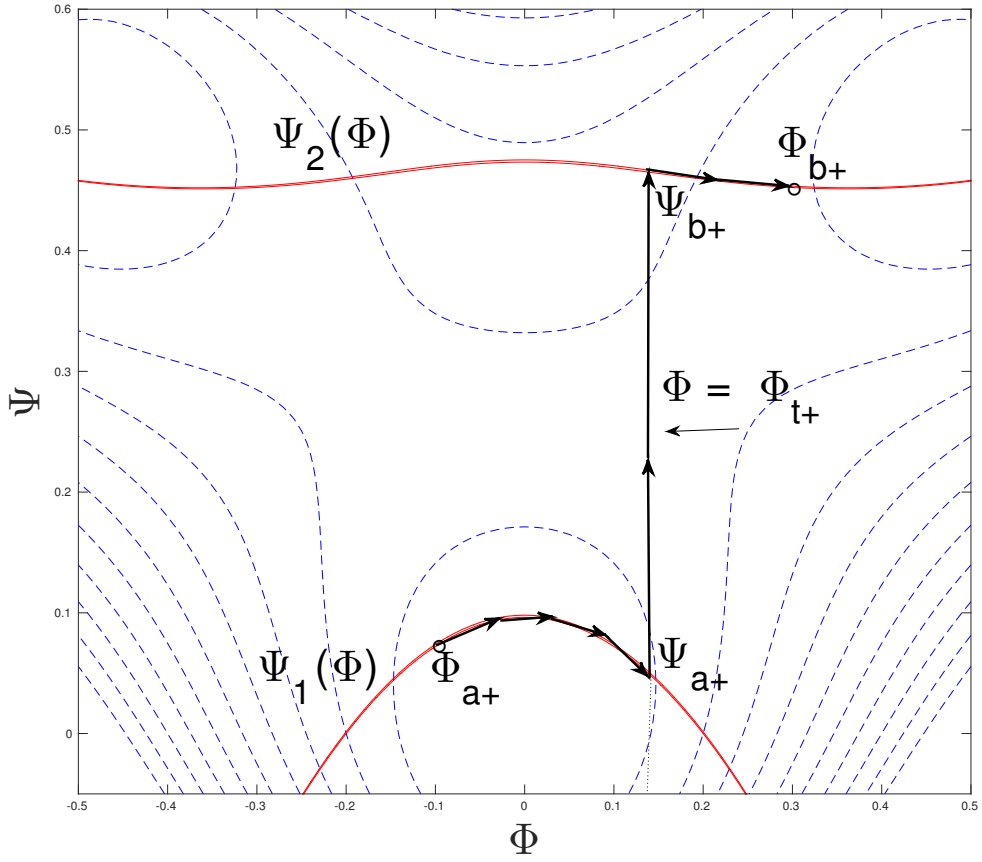

FIGURE 5. Contours of the potential $W(\Phi, \Psi)$ (blue/dotted) and nullclines $\Psi_{1,2}$ (red/solid). The arrows represent the trajectory of the composite internal layer. The region II solutions are along the nullclines and the vertical arrows represent the region III layer.

μ is achieved (faster scales would lead to inconsistencies and slower ones would simply give a time-independent problem).

Defining $\mu(y) = -\Phi_{yy} + \tilde{W}'(\Phi)$ and expanding $\mu = \mu_0 + \epsilon_{11}\mu_1 + O(\epsilon_{11}^2)$ leads to

$$-\frac{dx_j}{dt}\Phi_{0y} = (\mu_1)_{yy}. \tag{18}$$

In region III, $\mu_{1zz} = 0$, and therefore μ_1 is continuously differentiable throughout region II. Asymptotic matching conditions at the next order in the expansion (c.f. [24] or [23]) mean that the derivative of $\mu_1(y)$ matches the derivative of the outer leading order solution $\mu_0(x) \equiv \tilde{W}'(\Phi(x))$, and therefore

$$\mu_{1y}(\pm\infty) = \lim_{x \to x_j \pm} (\tilde{W}'(\Phi))_x$$

where on the right $\Phi = \Phi(x)$ is the leading order solution in regions I and IV. It follows from integration of (18) that the interface velocity satisfies

$$\frac{dx_j}{dt} = -\frac{\left[\tilde{W}'(\Phi)_x\right]_j}{[\Phi]_j}$$

where the notation $[f]_j = \lim_{x\to x_j^+} f(x) - \lim_{x\to x_j^-} f(x)$ will be used throughout. We will also use the notation $f(x_j^\pm)$ to denote the limits from the left and right at the interfaces.

2.4. **Free boundary problem.** The calculation made above can be summarized as a free boundary problem. We suppose that a multilayered solution has N internal domains separated by interfaces located at x_j with $x_0 < x_1 < \ldots < x_N$. Without loss of generality, the sign of Φ alternates $+, -, +, -, \ldots$ between subdomains. The dynamic free boundary problem therefore reads

$$\text{(F1)} \qquad \Phi_t = \tilde{W}'(\Phi)_{xx} - \alpha\Phi, \quad x \neq x_j, \quad j = 0, 1, \ldots, N$$

$$\text{(F2)} \qquad \begin{aligned} &\lim_{x\to\pm\infty} \Phi = 0, \quad \Phi(x_0^-) = \Phi_{a+}, \quad \Phi(x_0^+) = \Phi_{b+}, \quad \Phi(x_N^-) = \Phi_{b\pm}, \quad \Phi(x_N^+) = \Phi_{a\pm}, \\ &\Phi(x_j^\pm) = \Phi_\pm, \quad j \text{ even}, \qquad \Phi(x_j^\pm) = \Phi_\mp, \quad j \text{ odd}, \end{aligned}$$

$$\text{(F3)} \qquad dx_j/dt = -[\tilde{W}'(\Phi)_x]_j/[\Phi]_j, \quad j = 0, 1, \ldots, N.$$

The subscript sign for boundary conditions at x_N is positive if N is odd and negative if N is even. The equilibrium free boundary problem is obtained by suppressing time derivatives, leading to

$$\text{(F1')} \qquad \tilde{W}'(\Phi)_{xx} = \alpha\Phi, \quad x \neq x_j, \quad j = 0, 1, \ldots, N$$

$$\text{(F3')} \qquad [\tilde{W}'(\Phi)_x]_j = 0, \quad j = 0, 1, \ldots, N.$$

We note that the interface relations (10) and (11) imply $\tilde{W}'$ is continuous across interfaces and

$$\tilde{W}'(x_j) = \frac{[\tilde{W}(\Phi)]_j}{[\Phi]_j}. \tag{19}$$

The problems (F1-F3) and (F1',F2,F3') serve as a point of departure for the remainder of the paper. Note that the independent variable can be scaled $x' = \sqrt{\alpha}x$ so as to eliminate the parameter α. Significantly, this means that $1/\sqrt{\alpha}$ defines a lengthscale proportional to the size of internal domains. Note this is different than the uncoupled Ohta-Kawasaki equation, where the domain size of energy minimizers scales like $\alpha^{-1/3}$ [22]. Because of the scale invariance, from this point forward α will be set to one.

2.5. **Limiting free energy.** A natural candidate for the sharp interface free energy can be obtained by replacing W with $\tilde{W}$ and suppressing gradient terms in (2), leading to

$$E_0(\Phi) = \int_{\mathbb{R}} \frac{1}{2}(v_x)^2 + \tilde{W}(\Phi) - \tilde{W}(0)\, dx, \quad v_{xx} = \Phi, \quad \lim_{x\to\pm\infty} v = 0. \tag{20}$$

This is restricted to Φ in the admissible class

$$\mathcal{A} = \left\{ \Phi \in L^2(\mathbb{R}) \,|\, \text{there exists } x_0 < x_1 < \ldots < x_N \text{ so that } \Phi \in C^2(\mathbb{R}/\{x_j\}) \text{ and } \Phi \text{ satisfies (F2)} \right\}.$$

It can be shown that E_0 is a Lyapunov function for the free boundary evolution.

Proposition 1. *Suppose that $\Phi(\cdot, t) \in \mathcal{A}$ for $t \in \mathbb{R}^+$, and Φ is a solution to (F1-F3). Then $dE_0/dt \leq 0$, where equality holds only when Φ satisfies (F1',F2,F3').*

Proof. Write

$$E_0(\Phi) = \sum_{j=0}^{N+1} \int_{x_{j-1}}^{x_j} \frac{1}{2}(v_x)^2 + \tilde{W}(\Phi)\, dx \tag{21}$$

where $x_{-1} = -\infty$ and $x_{N+1} = +\infty$. A direct calculation gives

$$\frac{dE_0}{dt} = \sum_{j=0}^{N+1} \int_{x_{j-1}}^{x_j} v_x v_{xt} + \tilde{W}'(\Phi)\Phi_t\, dx - \sum_{j=0}^{N} [\tilde{W}(\Phi)]_j \frac{dx_j}{dt}. \tag{22}$$

Integration by parts on each subdomain produces

$$\int_{\mathbb{R}} v_x v_{xt}\, dx = -\sum_{j=0}^{N+1} \int_{x_{j-1}}^{x_j} v\Phi_t\, dx - \sum_{j=0}^{N} v(x_j)[v_{xt}]_j. \tag{23}$$

Because $\Phi_t = (\tilde{W}'(\Phi) - v)_{xx}$,

(24)

$$\begin{aligned}\frac{dE_0}{dt} &= \sum_{j=0}^{N+1} \int_{x_{j-1}}^{x_j} (\tilde{W}'(\Phi) - v)(\tilde{W}'(\Phi) - v)_{xx}\, dx - \left(\sum_{j=0}^{N} [\tilde{W}(\Phi)]_j \frac{dx_j}{dt} + v(x_j)[v_{xt}]_j \right) \\ &= -\sum_{j=0}^{N+1} \int_{x_{j-1}}^{x_j} ([\tilde{W}'(\Phi) - v]_x)^2\, dx - \left(\sum_{j=0}^{N} [\tilde{W}(\Phi)]_j \frac{dx_j}{dt} + v(x_j)[v_{xt}]_j + (\tilde{W}'(\Phi) - v)(x_j)[W'(\Phi)_x]_j \right).\end{aligned}$$

One finds

$$\begin{aligned}[v_{xt}]_j &= \lim_{\epsilon\to 0} v_{xt}(x_j + \epsilon, t) - v_{xt}(x_j - \epsilon, t) \\ &= \lim_{\epsilon\to 0} \frac{d}{dt}\Big(v_x(x_j(t) + \epsilon, t) - v_x(x_j(t) - \epsilon, t)\Big) - \Big(v_{xx}(x_j + \epsilon, t) - v_{xx}(x_j - \epsilon, t)\Big)\frac{dx_j}{dt} \\ &= \lim_{\epsilon\to 0} \frac{d}{dt} \int_{x_j - \epsilon}^{x_j + \epsilon} \Phi\, dx - [\Phi]_j \frac{dx_j}{dt}.\end{aligned} \tag{25}$$

Thanks to the boundedness of Φ_t (via equation F1) and the continuity of Φ on each subinterval,

(26)

$$\begin{aligned}&\lim_{\epsilon\to 0} \frac{d}{dt} \left(\int_{x_j}^{x_j+\epsilon} \Phi\, dx + \int_{x_j-\epsilon}^{x_j} \Phi\, dx \right) \\ &\quad = \lim_{\epsilon\to 0} \left(\int_{x_j}^{x_j+\epsilon} \Phi_t\, dx + \int_{x_j-\epsilon}^{x_j} \Phi_t\, dx + \Big(\Phi(x_j + \epsilon) - \Phi(x_j^+) + \Phi(x_j^-) - \Phi(x_j - \epsilon)\Big)\frac{dx_j}{dt} \right) = 0,\end{aligned}$$

and it follows that $[v_{xt}]_j = -[\Phi]_j \frac{dx_j}{dt}$. Using this, the interface motion condition (F3) and the relations (19) give

$$\frac{dE_0}{dt} = -\sum_{j=0}^{N+1} \int_{x_{j-1}}^{x_j} ([\tilde{W}'(\Phi) - v]_x)^2\, dx. \tag{27}$$

If $dE_0/dt = 0$ then $\tilde{W}'(\Phi) - v$ must be a constant on each subdomain. This implies that both $\Phi_t = 0$ and $dx_j/dt = -[\tilde{W}'(\Phi)_x]_j/[\Phi]_j = 0$. □

3. Construction of multilayered equilibria

We now address the existence of solutions to the problem (F1',F2,F3'). This is done by first reformulating the problem by a change of variables which stems from Legendre transforms of each convex part of the effective potential $\tilde{W}$. To this end it is convenient to define C^2 convex extensions (see figure 3), called W_+, W_-, and W_0 so that

$$W_+(\Phi) = \tilde{W}(\Phi), \quad \Phi > \Phi_{t+} \tag{28}$$

$$W_-(\Phi) = \tilde{W}(\Phi), \quad \Phi < \Phi_{t-} \tag{29}$$

$$W_0(\Phi) = \tilde{W}(\Phi), \quad \Phi_{t-} < \Phi < \Phi_{t+} \tag{30}$$

The domains of $W_{+,-,0}$ can be extended to the whole real line so that $W'_{+,-,0}$ are one-to-one mappings from $\mathbb{R}$ to $\mathbb{R}$. The Legendre transforms $U_{+,-,0}$ are convex functions defined via

$$U_+(\mu) = \mu\Phi - W_+(\Phi), \quad \Phi = (W'_+)^{-1}(\mu), \tag{31}$$

with similar definitions for U_- and U_0. The inverse transforms are given by $W_{0,\pm}(\Phi) = \mu\Phi - U_{0,\pm}(\mu)$ and imply $\Phi = U'_{0,\pm}(\mu)$. The interface boundary conditions can be written using (10) and (11) as

$$U_0(\mu_{\Phi\pm}) = \mu_{\Phi_\pm}\Phi_{a\pm} - \tilde{W}(\Phi_{a\pm}) = \mu_{\Phi\pm}\Phi_\pm - \tilde{W}(\Phi_{b\pm}) = U_\pm(\mu_{\Phi\pm}), \quad U_+(\mu_\Phi) = U_-(\mu_\Phi). \tag{32}$$

They also imply that μ is continuous across edge interfaces x_0 and x_N, taking values $\mu = \tilde{W}'(\Phi_{a\pm}) = \tilde{W}'(\Phi_{b\pm}) = \mu_{\Phi\pm}$ at these points. At infinity, $\mu \to \tilde{W}'(0) \equiv \mu_\infty$.

The free boundary problem (F1',F2,F3') can now be reformulated as

$$\mu_{xx} = \begin{cases} U'_+(\mu) & x \in (x_j, x_{j+1}), \quad 0 \le j \le N,\ j \text{ even} \\ U'_-(\mu) & x \in (x_j, x_{j+1}), \quad 0 \le j \le N,\ j \text{ odd} \\ U'_0(\mu) & x < x_0 \text{ or } x > x_N \end{cases} \tag{33}$$

$$\lim_{x\to\pm\infty} \mu = \mu_\infty, \quad \mu(x_0) = \mu_{\Phi+}, \quad \mu(x_N) = \mu_{\Phi\pm}, \quad \mu(x_j) = \mu_\Phi, \quad j = 1, \ldots, N-1 \tag{34}$$

$$\lim_{x\to x_j^+} \mu_x = \lim_{x\to x_j^-} \mu_x, \quad j = 0, 1, \ldots, N. \tag{35}$$

Note by virtue of (19), $\mu(x)$ will be continuously differentiable throughout $\mathbb{R}$.

The solution to (33) on each subdomain is now straightforward. In the region $x < x_0$, the phase plane for this equation has a single saddle at $(\mu_\infty, 0)$ (see figure 6). The desired solution is along the unstable manifold where $\mu_{\Phi+} < \mu < \mu_\infty$ and $\mu_x < 0$. The first integral of (33) defines this curve implicitly as

$$\frac{1}{2}(\mu_x)^2 = U_0(\mu) - U_0(\mu_\infty). \tag{36}$$

For the edge domain $x_0 < x < x_1$, the phase plane has a saddle at μ_{s+}, where $U'_+(\mu_{s+}) = 0$. The corresponding value is $\Phi = 0$, and therefore $\mu_{s+} = W'_+(0)$. Since the convex extension W_+ for $\Phi < \Phi_{t+}$ is arbitrary, one can always ensure that $\mu_{s+} < \mu_{\Phi+}$ by choosing $W'_+(0)$ sufficiently negative. Note that on the interval $\mu > \mu_{s+}$, $U_+(\mu)$ is strictly increasing and has a unique inverse $U_+^{-1}(\eta)$ for $\eta > U_+(\mu_{s+})$. The solution to (33) satisfying (35) for $j = 0$ is therefore given implicitly by

$$\frac{1}{2}(\mu_x)^2 = U_+(\mu) + \frac{1}{2}(\mu_x)^2(x_0) - U_+(\mu_{\Phi+}) = U_+(\mu) - U_0(\mu_\infty), \tag{37}$$

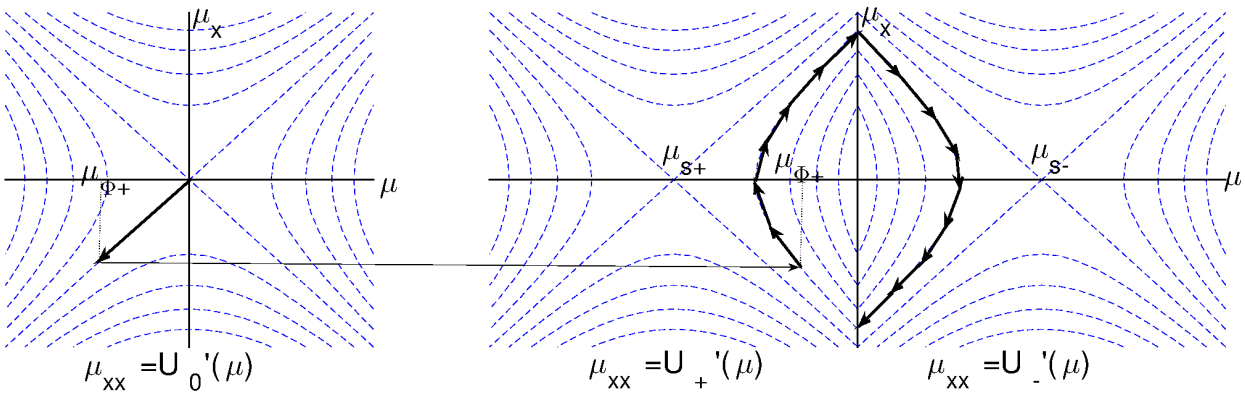

FIGURE 6. Left: phase plane contours for the exterior domains $x < x_0$ and $x > x_N$ (blue/dotted), and the solution curve for the domain $x < x_0$ (here $\mu_\infty = 0$). Right: phase plane contours for interior domains, where the equation $\mu_{xx} = U'_+$ is used for the portion left of the μ_x axis, and $\mu_{xx} = U'_-$ is used to the right. Also shown are solution curves (arrows) for $x_0 < x < x_1$ (left part) and $x_1 < x < x_2$ (right part). In these figures μ_∞ and μ_Φ are both zero.

where the last equality follows from (32) and (36). By the preceding observation, the desired solution curve can be written as a graph over the phase plane variable $\nu \equiv \mu_x$ as

$$\mu = U_+^{-1}\Big(\frac{1}{2}\nu^2 + U_0(\mu_\infty)\Big), \quad \sqrt{2[U_+(\mu_{\Phi+}) - U_0(\mu_\infty)]} < \nu < \sqrt{2(U_+(\mu_\Phi) - U_0(\mu_\infty))}.$$

Since $d\nu/dx = U'_+(\mu)$, the domain size is given via

$$x_1 - x_0 = \int_{x_0}^{x_1} dx = \int_{\sqrt{2[U_+(\mu_{\Phi+})-U_0(\mu_\infty)]}}^{\sqrt{2(U_+(\mu_\Phi)-U_0(\mu_\infty))}} \frac{d\nu}{U'_+(\mu(\nu))}. \tag{38}$$

For the domain $x_1 < x < x_2$, the phase plane has a saddle at $\mu_{s-} > 0$ (see figure 6), and therefore for $\mu < \mu_{s-}$, $U_-(\mu)$ is strictly decreasing with an inverse whose domain is $\eta > U_-(\mu_s)$. As in the preceding case, the solution is obtained implicitly as

$$\frac{1}{2}(\mu_x)^2 = U_-(\mu) + \frac{1}{2}(\mu_x)^2(x_1) - U_-(\mu_\Phi) = U_-(\mu) + \frac{1}{2}(\mu_x)^2(x_1) - U_+(\mu_\Phi) = U_-(\mu) - U_0(\mu_\infty). \tag{39}$$

where (32) and (37) were used. By induction, solutions for domains $x_j < x < x_{j+1}$ have the implicit form

$$\frac{1}{2}(\mu_x)^2 = U_\pm(\mu) - U_0(\mu_\infty), \tag{40}$$

where $+$ is chosen for j even and $-$ for j odd. Finally, for $x > x_N$, the solution is along the stable manifold of the saddle of $\mu_{xx} = U'_0(\mu)$. Since

$$\lim_{x\to x_N+} \frac{1}{2}(\mu_x)^2 = U_0(\mu_{\Phi\pm}) - U_0(\mu_\infty) = U_\pm(\mu_{\Phi\pm}) - U_0(\mu_\infty) = \lim_{x\to x_N-} \frac{1}{2}(\mu_x)^2,$$

an appropriate choice of sign of μ will ensure that μ_x is continuous at x_N, i.e. that (35) holds for all j.

Finally, we address the issue of returning to the Φ variables. Provided $\Phi = U'_{0,\pm}(\mu)$ is in the domain of the proper convex part of $\tilde{W}$, then a solution of (33-35) can be transformed back to a solution of (F1',F2,F3'). For the exterior domains $x < x_0$ and $x > x_N$, the maximum value of μ is achieved at $\mu = \mu_{\Phi\pm}$, which corresponds to the values $\Phi = U'_0(\mu_{\Phi\pm}) = \Phi_{a\pm}$. From the definition of $\Phi_{a\pm}$ in property P3, it follows that $\Phi = U'_0(\mu) \in (\Phi_{t-}, \Phi_{t+})$. For interior

domains which use U_+, $\mu_{min} \le \mu < \mu_\Phi$ and the minimum value is achieved (by using (40)) where $U_+(\mu_{min}) = U_0(\mu_\infty)$. It follows from the Legendre transform relations that $U_+(\mu_{min}) = \mu_{min}\Phi_{min} - W_+(\Phi_{min})$ and $U_0(\mu_\infty) = -W_0(0)$, where $\Phi_{min} \equiv U_+'(\mu_{min})$. As a consequence

$$W_+(\Phi_{min}) = \mu_{min}\Phi_{min} + W_0(0) < W_0(0),$$

since $\Phi_{min} > 0$ and $\mu_{min} < 0$ in this case. By the definition of $\tilde{W}$, this can only happen when $\Phi > \Phi_{t+}$. A similar argument shows that $\Phi < \Phi_{t-}$ for domains using U_-. The argument above can be summarized:

Theorem 1. *Provided $0 < \mu_\Psi < \mu_\Psi^{max}$, there is an equilibrium solution with $N+1$ interfaces solving (F1',F2,F3').*

4. Stability of multilayered solutions

We now address the question of whether equilibrium solutions are local minimizers of the effective free energy E_0. First, the second variation of the energy is shown to represent a non-negative quadratic form. This result is then used to develop rigorous bounds which show that equilibria have lower energy than nearby admissible states.

4.1. **Second variation.**

The second variation of the energy (20) can be computed formally from expanding Φ, v, and interface locations x_j. The resulting expression is analyzed to obtain a non-negativity result.

Let Φ_0 be an equilibrium solution with $N+1$ interfaces located at positions x_j. Denote by v_0 the corresponding nonlocal potential so that $v_{0xx} = \Phi_0$ and $v_0(\pm\infty) = 0$. Consider small perturbations of both interface locations $x_j' = x_j + \varepsilon\tilde{x}_j$ and perturbations of Φ away from interfaces of the form $\Phi = \Phi_0 + \varepsilon\tilde{\Phi}$. The total perturbation of Φ combines $\tilde{\Phi}$ and distributional contributions arising from moving discontinuities:

$$\Phi = \Phi_0 + \varepsilon\tilde{\Phi} - \varepsilon\sum_{j=0}^{N}[\Phi_0]_j\tilde{x}_j\delta(x - x_j).$$

Expanding the potential $v = v_0 + \varepsilon\tilde{v}$, one has

$$\tilde{v}_{xx} = \tilde{\Phi} - \sum_{j=0}^{N}[\Phi_0]_j\tilde{x}_j\delta(x - x_j).$$

Substituting into E_0 in (20) and identifying terms proportional to ε^2 results in a quadratic expression representing the second variation of the energy

$$\sum_{j=0}^{N+1}\frac{1}{2}\int_{x_{j-1}}^{x_j}\tilde{W}''(\Phi_0)\tilde{\Phi}^2 + \tilde{v}^2 dx + \frac{1}{2}\sum_{j=0}^{N}v_{0x}(x_j)[\Phi_0]_j\tilde{x}_j^2. \tag{41}$$

It is convenient to reformulate this expression in terms of the variable $u \equiv \tilde{v}_x$ so that $u_x = \tilde{\Phi}$ away from interfaces. This results in the quadratic form

$$F(u,u) = \frac{1}{2}\int_{\mathbb{R}}P(u_x)^2 + u^2\,dx - \frac{1}{2}\sum_{j=0}^{N}\beta_j\delta_j^2, \quad \delta_j = [u]_j, \tag{42}$$

where

$$P \equiv \tilde{W}''(\Phi_0), \quad \beta_j \equiv -\frac{v_{0x}(x_j)}{[\Phi_0]_j} = -\frac{(P\Phi_0)(x_j)}{[\Phi_0]_j}, \quad \delta_j \equiv \tilde{x}_j[\Phi_0]_j. \tag{43}$$

so that $F(u,u)$ is the same as (41).

We will show that $F(u,u)$ is non-negative, and can only be zero if $\delta_j/[\Phi_0]_j$ are the same for all j, corresponding to perturbations which stem from uniform translation in space. The strategy is to first find a lower bound for fixed δ_j, by minimizing the quadratic functional subject to this constraint. The resulting finite dimensional quadratic form is then shown to be nonnegative.

The constrained minimizer u^* is given by the following linear problem

$$(Pu_x^*)_x = u^*, \quad [u^*]_j = \delta_j, \quad [Pu_x^*]_j = 0, \quad u^*(\pm\infty) = 0. \tag{44}$$

The construction of u^* proceeds as follows. The second order equation $(Pu_x)_x - u = 0$ has two linearly independent solutions, $u = \Phi_0$ and by reduction of order,

$$u = \Phi_1 \equiv c(x)\Phi_0(x), \quad c(x) = \int^x \frac{dx}{P\Phi_0^2}, \tag{45}$$

where the lower bound of the integral can be chosen arbitrarily. Now set

$$u(x) = \begin{cases} a_0\Phi_0, & x < x_0 \\ a_j\Phi_0 + b_j\Phi_1, & x_{j-1} < x < x_j, \quad j = 1,2,\dots,N \\ a_{N+1}\Phi_0, & x > x_N. \end{cases} \tag{46}$$

Proposition 2. *There exists a unique solution to (44) having the form (46).*

Proof. For any function u defined by (46), let $\gamma_j \equiv [Pu_x]_j$. Then

$$(a_0, a_1, \dots, a_{N+1}, b_1, b_2, \dots, b_N) \to (\delta_0, \delta_1, \dots, \delta_N, \gamma_0, \gamma_1, \dots, \gamma_N) \tag{47}$$

is a linear mapping from $\mathbb{R}^{2N+2} \to \mathbb{R}^{2N+2}$. It suffices to show that this mapping has a trivial kernel. Suppose a function $u(x)$ of the form (46) yields $\gamma_j = 0$ for all j. Then the function defined by (46) solves (44a) and is in $C^1(\mathbb{R})$. Multiplying the equation in (44) by u and integrating results in

$$\int_{\mathbb{R}} u^2 + P(u_x)^2\, dx = 0.$$

It follows that $u \equiv 0$ so that $a_j = 0 = b_j$ for all j. □

We may now show that u^* provides a lower bound on F.

Proposition 3. *Suppose that $u \in H^1([x_j, x_{j+1}])$ for each j and $u \in C^0(\mathbb{R}/\{x_j\})$. Let $\delta_j = [u]_j$ and define u^* as above. Then $F(u,u) \geq F(u^*,u^*)$.*

Proof. From the definition of F and integration by parts,

$$F(u,u) - F(u^*,u^*) = \frac{1}{2}\int_{\mathbb{R}} (u-u^*)^2 + P(u-u^*)_x^2 dx + \int_{\mathbb{R}} (u-u^*)u^* + (u-u^*)_x Pu_x^*\, dx \tag{48}$$

$$\geq \int_{\mathbb{R}} (u-u^*)\Big(u^* - (Pu_x^*)_x\Big)\, dx - \sum_{j=0}^{N} [P(u-u^*)u_x^*]_j = 0. \tag{49}$$

□

The lower bound $F(u^*,u^*)$ can be written explicitly in terms of $\{\delta_j\}$. From integration by parts on each subdomain, the remaining integral vanishes and we are left with boundary terms only,

$$F(u^*,u^*) = -\frac{1}{2}\sum_{j=0}^{N} \beta_j\delta_j^2 + (Pu_x^*)(x_j)[u^*]_j \equiv \frac{1}{2}\sum_{j=0}^{N} Q_j\delta_j,$$

where Q is a linear mapping from $\mathbb{R}^{N+1} \to \mathbb{R}^{N+1}$ defined by

$$Q_j(\delta_0, \delta_1, \dots, \delta_N) = -(a_{j+1}P\Phi_{0x} + b_{j+1}P\Phi_{1x})(x_j^+) - \beta_j\delta_j = -(a_jP\Phi_{0x} + b_jP\Phi_{1x})(x_j^-) - \beta_j\delta_j, \tag{50}$$

for $j = 0, 1, 2, \ldots$ and $b_0 = 0 = b_{N+1}$. Note that the coefficients a_j, b_j are implicitly linear functions of $(\delta_0, \delta_1, \ldots, \delta_N)$. For reasons of symmetry, it is helpful to rescale using $\Delta_j = \sqrt{\beta_j}\delta_j$ so that

$$F(u^*, u^*) = \frac{1}{2}\sum_{j=0}^{N} Q'_j \Delta_j, \quad Q'_j(\Delta) = \frac{Q(\Delta_0/\sqrt{\beta_0}, \Delta_1/\sqrt{\beta_1}, \ldots)}{\sqrt{\beta_j}}. \tag{51}$$

Proposition 4. *The quadratic form given by (51) is non-negative. Moreover, it is only zero when Δ is proportional to the translational eigenvector with components $\Delta_j = \sqrt{\beta_j}[\Phi_0]_j$.*

Proof. Step 1 (eigenvalue problem for Q'). Let λ be an eigenvalue for Q' and let Δ_j be components of the corresponding eigenvector. There is a corresponding solution to (44) of form (46) with $\delta_j = \Delta_j/\sqrt{\beta_j}$, with coefficients still labeled a_j, b_j. The interface conditions on u imply

$$a_{j+1}\Phi_0(x_j^+) + b_{j+1}\Phi_1(x_j^+) - a_j\Phi_0(x_j^-) + b_j\Phi_1(x_j^-) = \frac{\Delta_j}{\sqrt{\beta_j}}. \tag{52}$$

From definition (50), λ is an eigenvalue of Q' if

$$(a_{j+1}P\Phi_{0x} + b_{j+1}P\Phi_{1x})(x_j^+) = -(\lambda+1)\Delta_j\sqrt{\beta_j} = (a_jP\Phi_{0x} + b_jP\Phi_{1x})(x_j^-), \quad j = 0, 1, 2, \ldots, N. \tag{53}$$

These equations represent linear systems for each pair (a_j, b_j), whose solutions are

$$a_j = -\frac{\lambda+1}{D_j}\Big((P\Phi'_1)(x_{j-1}^+)\sqrt{\beta_j}\Delta_j - (P\Phi'_1)(x_j^-)\sqrt{\beta_{j-1}}\Delta_{j-1}\Big) \tag{54}$$

$$b_j = -\frac{\lambda+1}{D_j}\Big((P\Phi'_0)(x_j^-)\sqrt{\beta_{j-1}}\Delta_{j-1} - (P\Phi'_0)(x_{j-1}^+)\sqrt{\beta_j}\Delta_j\Big) \tag{55}$$

where

$$\begin{aligned} D_j =& (P\Phi'_0)(x_j^-)(P\Phi'_1)(x_{j-1}^+) - (P\Phi'_0)(x_{j-1}^+)(P\Phi'_1)(x_j^-) \\ =& \Big(c(x_{j-1}) - c(x_j)\Big)(P\Phi'_0)(x_j^-)(P\Phi'_0)(x_{j-1}^+) + \frac{(P\Phi'_0)(x_j^-)}{\Phi_0(x_{j-1}^+)} - \frac{(P\Phi'_0)(x_{j-1}^+)}{\Phi_0(x_j^-)}, \end{aligned} \tag{56}$$

where the latter results from (45). Since $(P\Phi'_0)(x_j^-)$ and $\Phi_0(x_{j-1}^+)$ have the same sign, $(P\Phi'_0)(x_{j-1}^+)$ and $\Phi_0(x_j^-)$ have opposite signs, and $c(x)$ is increasing, it follows that $D_j > 0$ for every j. In addition, equations (53) imply

$$a_0 = -\frac{(\lambda+1)\Delta_0\sqrt{\beta_0}}{(P\Phi'_0)(x_0^+))}, \quad a_n = -\frac{(\lambda+1)\Delta_N\sqrt{\beta_N}}{(P\Phi'_0)(x_N^-)}.$$

Inserting (54-55) into (52) leads to a system of equations

$$\begin{aligned} -\frac{\Delta_j}{(\lambda+1)\sqrt{\beta_j}} =& \frac{\Phi_0(x_j^+)}{D_{j+1}}\Big((P\Phi'_1)(x_j^+)\sqrt{\beta_{j+1}}\Delta_{j+1} - (P\Phi'_1)(x_{j+1}^-)\sqrt{\beta_j}\Delta_j\Big) \\ &+ \frac{\Phi_1(x_j^+)}{D_{j+1}}\Big((P\Phi'_0)(x_{j+1}^-)\sqrt{\beta_{j+1}}\Delta_j - (P\Phi'_0)(x_j^+)\sqrt{\beta_{j+1}}\Delta_{j+1}\Big) \\ &- \frac{\Phi_0(x_j^-)}{D_j}\Big((P\Phi'_1)(x_{j-1}^+)\sqrt{\beta_j}\Delta_j - (P\Phi'_1)(x_j^-)\sqrt{\beta_{j-1}}\Delta_{j-1}\Big) \\ &- \frac{\Phi_1(x_j^-)}{D_j}\Big((P\Phi'_0)(x_j^-)\sqrt{\beta_{j-1}}\Delta_{j-1} - (P\Phi'_0)(x_{j-1}^+)\sqrt{\beta_j}\Delta_j\Big), \end{aligned} \tag{57}$$

for $j = 1, 2, \dots, N-1$, with similar expressions for $j = 0, N$. Thanks to the identity $\Phi_0 P \Phi_1' - \Phi_1 P \Phi_0' = 1$ which is easily derived from (45), the coefficients in (57) simplify considerably, leading to a symmetric system

$$M\Delta = \frac{\lambda}{\lambda+1}\Delta, \quad M = \begin{pmatrix} d_0 & c_0 & & & \\ c_0 & d_1 & c_1 & & \\ & c_1 & d_2 & \ddots & \\ & & \ddots & \ddots & c_{n-1} \\ & & & c_{n-1} & d_n \end{pmatrix}, \quad \Delta = \begin{pmatrix} \Delta_0 \\ \Delta_1 \\ \vdots \\ \Delta_N \end{pmatrix} \tag{58}$$

where

$$d_j = -\frac{\beta_{j+1}[\Phi_0]_{j+1}}{[\Phi_0]_j D_{j+1}} - \frac{\beta_{j-1}[\Phi_0]_{j-1}}{[\Phi_0]_j D_j}, \quad j = 1, 2, \dots, N-1 \tag{59}$$

$$c_j = \frac{\sqrt{\beta_j \beta_{j+1}}}{D_{j+1}}, \quad j = 0, 1, \dots, N-1 \tag{60}$$

and

$$d_0 = -\frac{\beta_1[\Phi_0]_1}{[\Phi_0]_0 D_1}, \quad d_N = -\frac{\beta_{N-1}[\Phi_0]_{N-1}}{[\Phi_0]_N D_N}.$$

Showing that $\lambda \geq 0$ is therefore equivalent to showing that the eigenvalues of M are in $[0, 1]$.

Step 2 (eigenvalues of M). The quadratic form associated with M simplifies into the compact expression

$$M\Delta \cdot \Delta = \sum_{j=0}^{n-1} \frac{1}{D_{j+1}} \left(\sqrt{\frac{-\beta_{j+1}[\Phi_0]_{j+1}}{[\Phi_0]_j}} \Delta_j + \sqrt{\frac{-\beta_j[\Phi_0]_j}{[\Phi_0]_{j+1}}} \Delta_{j+1} \right)^2,$$

and therefore the eigenvalues of M are non-negative. Applying the inequality $2\sqrt{\beta_j \beta_{j+1}} v_j v_{j+1} \leq \beta_{j+1} v_j^2 + \beta_j v_{j+1}^2$, it follows that

$$M\Delta \cdot \Delta \leq \sum_{j=2}^{N-2} 2 d_j \Delta_j^2 + M_L \begin{pmatrix} \Delta_0 \\ \Delta_1 \end{pmatrix} \cdot \begin{pmatrix} \Delta_0 & \Delta_1 \end{pmatrix} + M_R \begin{pmatrix} \Delta_N \\ \Delta_{N-1} \end{pmatrix} \cdot \begin{pmatrix} \Delta_N & \Delta_{N-1} \end{pmatrix}, \tag{61}$$

where

$$M_L = \begin{pmatrix} -\frac{\beta_1[\Phi_0]_1}{D_1[\Phi_0]_0} & \frac{\sqrt{\beta_1\beta_0}}{D_1} \\ \frac{\sqrt{\beta_1\beta_0}}{D_1} & -\frac{\beta_0[\Phi_0]_0}{D_1[\Phi_0]_1} - \frac{2\beta_2[\Phi_0]_2}{D_2[\Phi_0]_1} \end{pmatrix}, \quad M_R = \begin{pmatrix} -\frac{\beta_{N-1}[\Phi_0]_{N-1}}{D_{N-1}[\Phi_0]_N} & \frac{\sqrt{\beta_{N-1}\beta_N}}{D_1} \\ \frac{\sqrt{\beta_{N-1}\beta_N}}{D_1} & -\frac{\beta_N[\Phi_0]_N}{D_{N-1}[\Phi_0]_{N-1}} - \frac{2\beta_{N-2}[\Phi_0]_{N-2}}{D_{N-2}[\Phi_0]_{N-1}} \end{pmatrix}. \tag{62}$$

For $j = 2, 3, \dots, N-2$, the coefficients β_j, D_j, and jumps $[\Phi_0]_j$ are all the same. Expressions (56) and (43b) imply the bounds

$$\frac{D_{j+1}}{\beta_{j+1}} \geq 2 \left| \frac{[\Phi_0]_{j+1}}{\Phi_\pm} \right|, \quad \frac{D_j}{\beta_{j-1}} \geq 2 \left| \frac{[\Phi_0]_j}{\Phi_\mp} \right|, \tag{63}$$

where the signs $\pm, \mp$ alternate with j. It follows

$$d_j = -\frac{\beta_{j+1}[\Phi_0]_{j+1}}{[\Phi_0]_j D_{j+1}} - \frac{\beta_{j-1}[\Phi_0]_{j-1}}{[\Phi_0]_j D_j} \leq \frac{1}{2} \left| \frac{|\Phi_\pm| + |\Phi_\mp|}{[\Phi_0]_j} \right| = \frac{1}{2}. \tag{64}$$

We will subsequently show that M_L and M_R have eigenvalues of at most one, which together with (61) and (64) implies

$$M\Delta \cdot \Delta \leq \sum_{j=0}^{N} \Delta_j^2 \tag{65}$$

so that the eigenvalues of M are ≤ 1 as desired.

Step 3 (eigenvalues of M_L and M_R). For any symmetric matrix of the form $\begin{pmatrix} a & c \\ c & b \end{pmatrix}$, the larger eigenvalue is $\frac{1}{2}(a+b+\sqrt{(a-b)^2+c^2})$. By direct differentiation, this can be shown to be an increasing function of c. It follows that the largest eigenvalue of M_L is bounded from above by the largest eigenvalue of

$$M_L' = \begin{pmatrix} -\frac{\beta_1[\Phi_0]_1}{D_1[\Phi_0]_0} & \frac{\sqrt{\beta_1\beta_0}}{D_1} \\ \frac{\sqrt{\beta_1\beta_0}}{D_1} & -\frac{\beta_0[\Phi_0]_0}{D_1[\Phi_0]_1} + \left|\frac{\Phi_0(x_1^+)}{[\Phi_0]_1}\right| \end{pmatrix}$$

since from (63), $D_2 \geq 2\beta_1[\Phi_0]_2/|\Phi_0(x_1^+)|$.

Let T_M be the trace and D_M be the determinant of M_L'. An upper bound on T_M is established by using (56) which gives both

$$D_1 \geq \left|\frac{\beta_1[\Phi_0]_1}{\Phi_0(x_0^+)}\right|, \quad D_1 \geq \left|\frac{\beta_0[\Phi_0]_0}{\Phi_0(x_1^-)}\right|,$$

so that

$$T_M = -\frac{\beta_1[\Phi_0]_1}{D_1[\Phi_0]_0} - \frac{\beta_0[\Phi_0]_0}{D_1[\Phi_0]_1} + \left|\frac{\Phi_0(x_1^+)}{[\Phi_0]_1}\right| \leq 1 + \left|\frac{|\Phi_0(x_0^+)| + |\Phi_0(x_1^-)|}{[\Phi_0]_1}\right| \leq 2.$$

Using this, it is straightforward to show that the larger eigenvalue of M_L',

$$\frac{1}{2}\left(T_M + \sqrt{T_M^2 - 4D_M}\right) \leq 1,$$

if and only if $D_M + 1 \geq T_M$. Using

$$D_1 \geq \left|\frac{\beta_1[\Phi_0]_1}{\Phi_0(x_0^+)}\right| + \left|\frac{\beta_0[\Phi_0]_0}{\Phi_0(x_1^-)}\right|,$$

one has

$$\left|\frac{\beta_1\Phi_0(x_1^+)}{[\Phi_0]_0}\right| + D_1\left|\frac{\Phi_0(x_1^-)}{[\Phi_0]_1}\right| \geq \left|\frac{\beta_1(\Phi_0(x_1^+)+\Phi_0(x_1^-))}{[\Phi_0]_0}\right| + \left|\frac{\beta_0[\Phi_0]_0}{[\Phi_0]_1}\right| = \left|\frac{\beta_1[\Phi_0]_1}{[\Phi_0]_0}\right| + \left|\frac{\beta_0[\Phi_0]_0}{[\Phi_0]_1}\right|.$$

Writing $|\Phi(x_1^-)/[\Phi_0]_1| = 1 - |\Phi(x_1^+)/[\Phi_0]_1|$ and dividing by D_1, we arrive at

$$\beta_1\left|\frac{\Phi_0(x_1^+)}{D_1[\Phi_0]_0}\right| + 1 \geq -\frac{\beta_1[\Phi_0]_1}{D_1[\Phi_0]_0} - \frac{\beta_0[\Phi_0]_0}{D_1[\Phi_0]_1} + \left|\frac{\Phi_0(x_1^+)}{[\Phi_0]_1}\right|, \tag{66}$$

which is precisely $D_M + 1 \geq T_M$. A similar calculation can be performed for M_R. This ensures that eigenvalues of M_L', M_L, and M itself all are bounded above by one, and $\lambda \geq 0$.

Step 4 (Uniqueness of the principal eigenvector of Q'). The eigenvalue $\lambda = 0$ corresponds to the zero eigenvalue of M. Supposing that $M\Delta = 0$, one can arbitrarily set $\Delta_0 = \sqrt{\beta_0}[\Phi_0]_0$, so that $\Delta_1 = -d_0/c_0 = \sqrt{\beta_1}[\Phi_0]_1$. The remaining components are determined uniquely from forward substitution by

$$\Delta_{j+1} = -(c_{j-1}\Delta_{j-1} + d_j\Delta_j)/c_j = \sqrt{\beta_{j+1}}[\Phi_0]_{j+1}. \tag{67}$$

□

Finally, a lower bound on $F(u,u)$ depending only on the interface displacements can be established.

Proposition 5. *Suppose that u satisfies the hypothesis of proposition 3, and $\delta_j = [u]_j = \tilde{x}_j/[\Phi_0]_j$. Provided*

$$\sum_{j=0}^{N} \beta_j \tilde{x}_j = 0, \tag{68}$$

there is a constant K so that

$$F(u,u) \geq K \sum_{j=0}^{N} \tilde{x}_j^2. \tag{69}$$

Proof. The condition (68) guarantees that the vector with components $\Delta_j = \sqrt{\beta_j}\delta_j$ is orthogonal to the nullspace of Q'. If $\lambda_1 > 0$ is the next smallest eigenvalue for Q' then

$$F(u,u) \geq F(u^*,u^*) \geq \frac{\lambda_1}{2} \sum_{j=0}^{N} \Delta_j^2 \geq \frac{\lambda_1}{2} \min_j \left(\frac{\beta_j}{[\Phi_0]_j^2} \right) \sum_{j=0}^{N} \tilde{x}_j^2.$$

□

4.2. **Equilibria as local minimizers.** We can now utilize the bound established in the previous section to show that equilibrium solutions are in fact local minimizers of the effective energy. This is done by first minimizing the energy subject to fixed interface locations. The energy of these constrained minimizers can then be estimated in terms of the second variation.

For interface positions $x_0' < x_1' < \ldots < x_N'$, consider the problem

$$\tilde{W}'(\Phi^*)_{xx} = \Phi^*, \quad [\tilde{W}'(\Phi^*)]_{x_j'} = 0, \quad [\tilde{W}'(\Phi^*)_x]_{x_j'} = 0, \quad \Phi^*(\pm\infty) = 0. \tag{70}$$

If $x_j' = x_j$ for all j, then a solution of (70) is just the equilibrium solution $\Phi^* = \Phi_0$. We can show that Φ^* provides a lower bound on the energy.

Proposition 6. *Suppose $\Phi \in \mathcal{A}$, with discontinuities at x_j', $j = 0, 1, \ldots, N$, and Φ^* satisfies (70). Then $E_0(\Phi^*) \leq E_0(\Phi)$.*

Proof. Let $v_{xx}^* = \Phi^*$ with $v^*(\pm\infty) = 0$. Using convexity of each term in E_0 and integrating by parts on each subinterval $x_j < x < x_{j+1}$ gives

$$E_0(\Phi) - E(\Phi^*) \geq \int_{\mathbb{R}} \tilde{W}'(\Phi^*)(\Phi - \Phi^*) + v_x^*(v - v^*)_x \, dx \tag{71}$$

$$= \int_{\mathbb{R}} \tilde{W}'(\Phi^*)(v - v^*)_{xx} - v_{xx}^*(v - v^*) \, dx \tag{72}$$

$$= \int_{\mathbb{R}} (\tilde{W}'(\Phi^*)_{xx} - \Phi^*)(v - v^*) \, dx \tag{73}$$

$$- \sum_{j=0}^{N} [\tilde{W}'(\Phi^*)]_{x_j'}(v - v^*)_x(x_j) - [\tilde{W}'(\Phi^*)_x]_{x_j'}(v - v^*)(x_j) = 0.$$

□

The construction of the constrained minimizers Φ^* can be accomplished by regarding x_j' as perturbations of the equilibrium interface locations x_j and applying an implicit function theorem argument. From this point on, the notation $O(\delta)$ is employed in a strict sense: if a quantity $Q(\Phi^*) = O(\delta)$ there exists some $C > 0$, independent of Φ^*, so that $|Q| < C\delta$ where $\delta \equiv \max_j |x_j' - x_j|$.

Proposition 7. *If $\delta \equiv \max_j |x'_j - x_j|$ is sufficiently small then (70) has a solution $\Phi^* \in L^2(\mathbb{R}) \cap C^1(\mathbb{R}/\{x'_j\})$. Moreover, for each interval $\max(x_j, x'_j) < x < \min(x_{j+1}, x'_{j+1})$, the estimate $\Phi^* - \Phi_0 = O(\delta)$ holds, and for intervals $x < \min(x_0, x'_0)$ and $x > \max(x_N, x'_N)$, there are constants C_1, C_2 so that*

$$|\Phi^* - \Phi_0| \le C_1 \delta \exp(-C_2|x|) \tag{74}$$

Proof. Step 1 (mapping to unperturbed interface locations). Let $\varphi(x) \in C_0^\infty(\mathbb{R})$ be some smooth function with support in $(-l, l)$, where $l = \frac{1}{4}\min_{i,j}|x_i - x_j|$ and where $\int_{\mathbb{R}} \varphi\, dx = 1$. A smooth change of variables is given by $x = g(x'; x'_0, x'_1, \ldots, x'_N)$ where g satisfies

$$g(x'; \cdot) = x' + x_0 - x'_0, \quad x' < x'_0 \tag{75}$$

$$\frac{dg}{dx'}(x'; \cdot) = 1 + \sum_{j=1}^{N-1} [(x_j - x_{j-1}) - (x'_j - x'_{j-1})]\varphi\Big(x' - (x'_j - x'_{j-1})/2\Big), \quad x' \ge x'_0 \tag{76}$$

Provided $\delta < l/2$, then $g_{x'} = 1$ in a neighborhood of each interface at x'_j. Since $g(x'_0) = x_0$, and in general $g(x'_j) - g(x'_{j-1}) = x_j - x_{j-1}$, by induction $g(x'_j) = x_j$ for all j. It is easily checked that

$$g_{x'} = 1 + O(\delta), \quad g_{x'x'} = O(\delta). \tag{77}$$

As in section 3, the problem (70) can be written in terms of the Legendre transform variable μ, giving

$$\mu_{xx} = U'(\mu), \quad [\mu]_{x_j} = 0, \quad [\mu_x]_{x_j} = 0, \quad \mu(\pm\infty) = 0, \tag{78}$$

where $U = U_0$ or $U_\pm$ depending on which subinterval x lies in. Applying the change of independent variable $x = g(x'; \cdot)$ means that $\mu(x) = \mu(g(x'))$ solves

$$\mu_{xx} = \frac{U'(\mu) - g_{x'x'}\mu_x}{g_{x'}^2} \equiv f(\mu, \mu_x, x), \tag{79}$$

where derivatives of g are evaluated at $x' = g^{-1}(x)$. Note that

$$f(\mu, \mu_x, x) = \begin{cases} U_0'(\mu) & x < x_0 \text{ or } x > x_N \\ U_\pm' + U_1(\mu, \mu_x, x) & x_0 < x < x_N \end{cases}$$

where $U_1 = O(\delta)$.

Step 2 (evolution of the unstable manifold's graph). The solution of (79) for $x < x_0$ or $x > x_N$ is a trajectory along the unstable and stable manifolds, M_u and M_s respectively, of the first order system

$$(\mu, \nu)_x = (\nu, U_0'(\mu)), \quad \nu \equiv \mu_x, \tag{80}$$

whereas for $x_0 < x < x_N$, the corresponding first order system is

$$(\mu, \nu)_x = (\nu, f(\mu, \nu, x)). \tag{81}$$

Finding a solution to (79) therefore involves showing the existence of a continuous solution $(\mu, \nu)(x)$ of (81) for which $(\mu, \nu)(x_0)$ and $(\mu, \nu)(x_N)$ are on M_u and M_s, respectively (see figure 7). Note that if the interface locations are unperturbed ($x'_j = x_j$ for all j), then the equilibrium solution $(\mu_0(x), \nu_0(x))$ where $\nu_0 = \mu_{0x}$ is such a trajectory.

For some open neighborhood $B \subset \mathbb{R}^2$ of $(\mu_0, \nu_0)(x_0)$, the unstable manifold is described by a smooth graph $\nu = h_0(\mu)$ where $h_0' > 0$. It will be shown that for each x, the set $T(x) =$

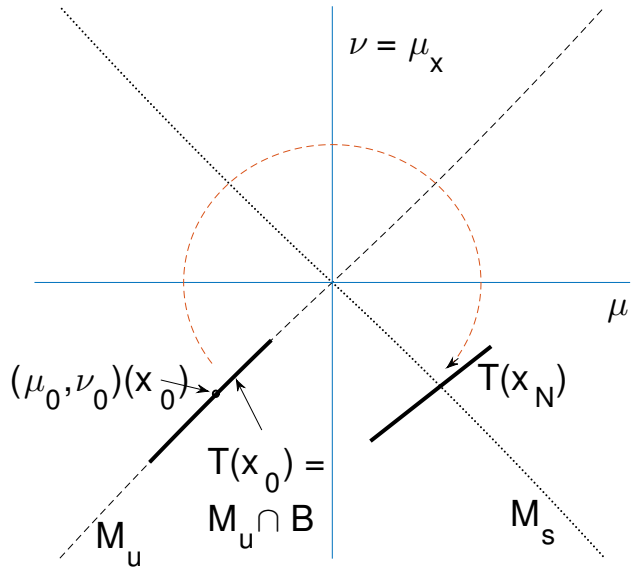

FIGURE 7. A local portion $T(x_0)$ of the unstable manifold M_u evolves according to (81) for $x_0 < x < x_N$. It is shown that $T(x)$ persists as a monotone increasing graph, and therefore must intersect the stable manifold M_s transversally.

$\{(\mu,\nu)(x)|(\mu,\nu)(x_0) \in M_u \cap B\}$ is the graph of $\nu(\mu) = h(\mu, x)$ where h solves a nonlinear transport equation

$$h_x + hh_\mu = f(\mu, h, x), \quad h(\mu, 0) = h_0(\mu). \tag{82}$$

A straightforward application of the method of characteristics reveals that characteristic curves solve $\mu_x = h$ and h evolves along characteristics as $\frac{d}{dx}h(\mu, x) = f(\mu, h, x)$, which is precisely the system (81) with $\nu(x) = h(\mu(x), x)$. It follows by standard theory that $h(\mu, x)$ exists on the domain $\{(x, \mu)|x_0 < x < x_N, \mu \in T_\mu(x)\}$, and is twice differentiable except possibly at the discrete values $x = x_j$. Differentiating (82) with respect to μ gives

$$h_{x\mu} + hh_{\mu\mu} + h_\mu^2 = f_\mu.$$

Using this fact, the slope of the graph h_μ evolves along trajectories as

$$\frac{d}{dx}h_\mu(\mu(x), x) = hh_{\mu\mu} + h_{x\mu} = f_\mu - h_\mu^2 = U''_\pm(\mu) + U_{1\mu} - h_\mu^2.$$

Since $U_1 = O(\delta)$ and $U_\pm$ are convex, if δ is small enough then $U_{1\mu} < U''_\pm(\mu)$. It follows that $dh_\mu/dx > -h_\mu^2$, and integration of this inequality gives

$$\frac{1}{h_\mu(\mu(x), x)} < \frac{1}{h_\mu(\mu(x_0), x_0)} + x - x_0,$$

which means that h_μ remains positive and $T(x_N)$ and M_s intersect transversally.

Step 3 (implicit function theorem). Solutions to (80-81) depend in a continuously differentiable fashion with respect to $x'_0, x'_1, \ldots$ via the dependence of U_1 on g. The stable manifold M_s can be written as a graph $\nu = h_s(\mu)$ where $h'_s < 0$. The function

$$q(\mu; x'_0, x'_1, \ldots, x'_N) = h(\mu, x_N; x'_0, x'_1, \ldots, x'_N) - h_s(\mu)$$

is defined on an open neighborhood of $\mu_0(x_N)$. From the previous step, it follows that $q_\mu > 0$ for μ close to $\mu_0(x_N)$ and $q(\mu_0(x_N), x_0, x_1, \ldots, x_N) = 0$. Provided δ is small enough, the implicit function theorem guarantees the existence of μ_N so that $q(\mu_N, x_0', x_1', \ldots, x_N') = 0$. This means the trajectory $\mu^*(x)$ with $\mu^*(x_N) = \mu_N$ will solve (79) throughout $\mathbb{R}$. In addition, $\mu_N - \mu_0(x_N) = O(\delta)$ so that $\mu^*(x) - \mu_0(x) = O(\delta)$ for $x_0 < x < x_N$.

Step 4 (returning to original variables). For each subinterval $x_j < x < x_{j+1}$, let $\Phi^{**}(x) = U'_{0,\pm}(\mu^*(x))$, where the choice of $\pm, 0$ corresponds to the subinterval type of the equilibrium solution. Then $\Phi^*(x) = \Phi^{**}(g(x))$ solves (70). On the interior intervals where $x_0 < x < x_N$, $\mu^* - \mu_0 = O(\delta)$ and therefore $\Phi^{**}(x) - \Phi_0 = O(\delta)$ also. For x between $\max(x_j, x_j')$ and $\min(x_{j+1}, x_{j+1}')$, both $\Phi^{**}(x)$ and $\Phi^*(x)$ are continuously differentiable, and (77a) implies

$$\Phi^*(x) - \Phi_0(x) = \Phi^{**}(g(x)) - \Phi_0(x) = \Phi^{**}(x) - \Phi_0(x) + O(\delta) = O(\delta).$$

For the exterior intervals $x < \min(x_0, x_0')$ and $x > \max(x_N, x_N')$, Φ_0 and Φ^* are the same up to translation. Therefore $\Phi^*(x) = \Phi_0(x + x_t)$ for some $x_t = O(\delta)$. It follows that

$$|(\Phi^* - \Phi_0)(x)| = |\Phi_0(x + x_t) - \Phi_0(x)| \le C_1 \delta |\Phi_{0x}(x)|$$

for some constant C_1. Since both μ_0 and Φ_0 decay exponentially in x as $|x| \to \pm\infty$, the estimate (74) follows. □

Theorem 2. *If $\delta = \max_j |x_j - x_j'|$ is sufficiently small, then for any $\Phi \in \mathcal{A}$ with jump discontinuities at $x_0', x_1', \ldots, x_N'$, $E_0(\Phi) \ge E_0(\Phi_0)$. Moreover, equality occurs only in the case where $\Phi(x) = \Phi_0(x + x_t)$ for some $x_t \in \mathbb{R}$.*

Proof. Step 1 (translation of Φ). Choose

$$x_t = \frac{\sum_{j=0}^N \beta_j (x_j' - x_j)}{\sum_{j=0}^N \beta_j},$$

so that if $\tilde{x} = x_j' - x_j - x_t$, (68) holds. Note that $x_t \le O(\delta)$ and therefore $\delta' \equiv \max_j |x_j' - x_j - x_t| \le 2\delta$.

Using proposition 6, it suffices to estimate $E_0(\Phi^*) - E_0(\Phi_0)$, where Φ^* has jump discontinuities at the translated interfaces $x_j' - x_t$. To simplify notation, we will replace $x_j' - x_t$ with x_j' in what follows. To estimate the integral in (20), $\mathbb{R}$ will be subdivided into 'interface" intervals $I_j = (\min(x_j, x_j'), \max(x_j, x_j'))$ and "subdomain" intervals $R_j = (\max(x_{j-1}, x_{j-1}'), \min(x_j, x_j'))$, where $x_{-1} = -\infty$ and $x_{N+1} = +\infty$.

Step 2 (estimates on R_j). By proposition 7, $\Phi^* - \Phi_0 = O(\delta')$ on each interior R_j, while (74) holds for intervals R_0 and R_{N+1}. Consequently, using $v^*_{xx} = \Phi^*$ and integration by parts,

$$\begin{aligned}
&\int_{R_j} \tilde{W}(\Phi^*) - \tilde{W}(\Phi_0) + \frac{1}{2}(v_x^* - v_{0x}^{*2})\, dx \\
&= \int_{R_j} \tilde{W}'(\Phi_0)(\Phi^* - \Phi_0) + \frac{1}{2}\tilde{W}''(\Phi_0)(\Phi^* - \Phi_0)^2 + \frac{1}{2}([v^* - v_0]_x)^2 + v_{0x}(v^* - v_0)_x\, dx + O(\delta'^3) \\
&= \int_{R_j} \Big(\tilde{W}'(\Phi_0) - v_0\Big)(\Phi^* - \Phi_0) + \frac{1}{2}\tilde{W}''(\Phi_0)(\Phi^* - \Phi_0)^2 + \frac{1}{2}([v^* - v_0]_x)^2\, dx + v_0(v^* - v_0)_x|_{x_j}^{x_{j+1}} + O(\delta'^3).
\end{aligned} \tag{83}$$

By virtue of $v_0 = \tilde{W}'(\Phi_0)$, the first term is zero.

Step 3 (estimates on I_j). Without loss of generality, suppose that $x_j' < x_j$ and Φ_0 is positive on the interval (x_j, x_{j+1}) so that $\tilde{W}$ and W_+ coincide. Expand

$$\Phi^*(x) = \Phi^*(x_j'^+) + \Phi_x^*(x_j'^+)(x - x_j') + O(\delta'^2) = \Phi_0(x_j^+) + (\Phi^* - \Phi_0)(x_j^+) + \Phi_x^*(x_j'^+)(x - x_j') + O(\delta'^2), \tag{84}$$

and

$$\Phi_0(x) = \Phi_0(x_j^-) + \Phi_{0x}(x_j^-)(x - x_j) + O(\delta'^2). \tag{85}$$

Using (84), (85), and the fact $v_0(x_j) = W'_{\pm}(\Phi_0(x_j^{\pm}))$,

$$\begin{aligned}
&\int_{I_j} W_+(\Phi^*) - W_-(\Phi_0)\,dx \\
&= \int_{I_j} W_+(\Phi_0(x_j^+)) - W_-(\Phi_0(x_j^-)) + v_0(x_j)\left[(\Phi^* - \Phi_0)(x_j^+) + \Phi^*_x(x_j^+)(x - x'_j) - \Phi_{0x}(x_j^-)(x - x_j)\right] dx + O(\delta'^3) \\
&= [\tilde{W}(\Phi_0)]_j(x_j - x'_j) + v_0(x_j)(\Phi^* - \Phi_0)(x_j^+)(x_j - x'_j) + \frac{1}{2}v_0(x_j)[\Phi^*_x(x_j^+) + \Phi'_{0x}(x_j^-)](x_j - x'_j)^2 + O(\delta'^3).
\end{aligned} \tag{86}$$

The nonlocal energy term in E_0 is estimated as

$$\begin{aligned}
\frac{1}{2}\int_{I_j} v_x^{*2} - v_{0x}^2\,dx &= \int_{I_j} \frac{1}{2}([v^* - v_0]_x)^2 + v_{0x}(v^* - v_0)_x\,dx \\
&\geq -\int_{I_j} v_0(\Phi^* - \Phi_0)\,dx + v_0(v^* - v_0)_x|_{x'_j}^{x_j}.
\end{aligned} \tag{87}$$

Note that the boundary terms will cancel those in (83). Expanding

$$v_0(x) = v_0(x_j) + v_{0x}(x_j)(x - x_j) + O(\delta'^2),$$

and using (84) and (85) gives

$$\begin{aligned}
\int_{I_j} v_0(\Phi^* - \Phi_0)\,dx =& v_0(x_j)[\Phi_0]_j(x_j - x'_j) + v_0(x_j)(\Phi^* - \Phi_0)(x_j^+)(x_j - x'_j) + \\
&\frac{1}{2}v_0(x_j)[\Phi^*_x(x_j^+) + \Phi_{0x}(x_j^-)](x_j - x'_j)^2 - \frac{1}{2}v_{0x}(x_j)[\Phi_0]_j(x_j - x'_j)^2 + O(\delta'^3).
\end{aligned} \tag{88}$$

Step 4 (Complete estimate). Combining (83),(86),(87) and (88) gives

$$E_0(\Phi^*) - E_0(\Phi_0) \geq \frac{1}{2}\int_{\cup_j R_j} W''(\Phi_0)(\Phi^* - \Phi_0)^2 + ([v^* - v_0]_x)^2\,dx + \frac{1}{2}\sum_{j=0}^{N} v_{0x}(x_j)[\Phi_0]_j(x'_j - x_j)^2 + O(\delta'^3). \tag{89}$$

Now define

$$u = \begin{cases} (v^* - v_0)_x & x \in \cup_j R_j \\ \left((v^* - v_0)_x(x_j) - [\Phi_0]_j(x_j - x'_j)\right)\frac{x - x'_j}{x_j - x'_j} + (v^* - v_0)_x(x'_j)\frac{x - x_j}{x'_j - x_j} & x \in I_j \end{cases} \tag{90}$$

Note that u is continuous on $\mathbb{R}/\{x_j\}$ and $[u]_j = [\Phi_0]_j(x_j - x'_j) \equiv \delta_j$, so that it fulfills the hypothesis of proposition 3.

We will now show that u and u_x are $O(\delta')$ on the I_j subintervals, and therefore

$$\frac{1}{2}\int_{\cup_j I_j} W''(\Phi_0)(u_x)^2 + u^2\,dx = O(\delta'^3). \tag{91}$$

Since $(v^* - v_0)_{xx} = \Phi^* - \Phi_0$, integration on R_0 and then I_1 gives $(v^* - v_0)_x = O(\delta')$ on these subintervals. Proceeding inductively, $(v^* - v_0)_x(x) = O(\delta')$ for all $x \in \mathbb{R}$, and in particular

$u = O(\delta')$ on each I_j. For any $x \in I_j$,

$$\begin{aligned} u_x(x) &= \frac{(v^* - v_0)_x(x_j) - (v^* - v_0)_x(x_j')}{x_j - x_j'} - [\Phi_0]_j \\ &= \frac{1}{x_j - x_j'} \int_{x_j'}^{x_j} (\Phi^* - \Phi_0)(x)\, dx - [\Phi_0]_j \\ &= \frac{[\Phi_0]_j (x_j - x_j') + O(\delta'^2)}{x_j - x_j'} - [\Phi_0]_j = O(\delta'), \end{aligned} \tag{92}$$

where the second to last equality follows from subtracting (84) and (85) to give $\Phi^* - \Phi_0 = [\Phi_0]_j + O(\delta')$.

Combining (89) and (91), it follows from proposition 5 that

$$\begin{aligned} E(\Phi) - E(\Phi_0) &\geq \frac{1}{2} \int_{\mathbb{R}} W''(\Phi_0)(u_x)^2 + u^2\, dx - \frac{1}{2} \sum_{j=0}^{N} \beta_j \delta_j^2 + O(\delta'^3) \\ &\geq K \sum_{j=0}^{N} (x_j' - x_j)^2 + O(\delta'^3) \geq K\delta'^2 + O(\delta'^3). \end{aligned} \tag{93}$$

At this point, δ', and therefore δ, can be chosen so that $E_0(\Phi) - E_0(\Phi_0) > 0$ unless $x_j' = x_j$ for all j. In this case, the convexity of the functional E_0 on each subinterval (x_j, x_{j+1}) implies that $E_0(\Phi) - E_0(\Phi_0) > 0$ unless $\Phi \equiv \Phi_0$. □

5. Discussion and conclusion

This work establishes the basic structure and properties of copolymer/solvent multilayers. It is, of course, not comprehensive in scope and suggests many further questions. A variety of connections to other studies and future prospects are discussed below.

5.1. **Comparison to the sharp interface model [12].** Our results should be contrasted with those of van Gennip and Peletier [12], who study global energy minimizers in a somewhat different sharp interface model of copolymer mixtures. Their model assumes that each subdomain exhibits only a pure phase, whereas ours allows for incomplete segregation, where some B-monomer is allowed to exist within an A-rich domain, for example. A second difference is that [12] employs a constraint for total polymer volume, which in our notation would read

$$\int_{-\infty}^{\infty} \Psi\, dx = M. \tag{94}$$

This is considerably different than specifying the far-field chemical potential μ_Ψ in the diffuse interface model. Indeed, if one was interested in minimizing (2) with constraint (94), it would be seen that there is no global minimizer at all. Consider the sequences

$$\Psi_n = \frac{M}{n} \begin{cases} 1 - |x/n|, & |x| < n \\ 0, & |x| > n \end{cases}$$

and $\Phi_n \equiv 0$. Since $W(\Phi, \Psi)$ is quadratic near the minimum at $(0,0)$, then $E(\Phi_n, \Psi_n) \sim 1/n$ as $n \to \infty$. The infimum of E is therefore zero under this constraint, but the minimum approached by the minimizing sequence $\{\Phi_n, \Psi_n\}$ cannot be obtained. This is reflective of physical reality: if a finite volume of polymer was placed in an infinite domain of solvent, the free energy would

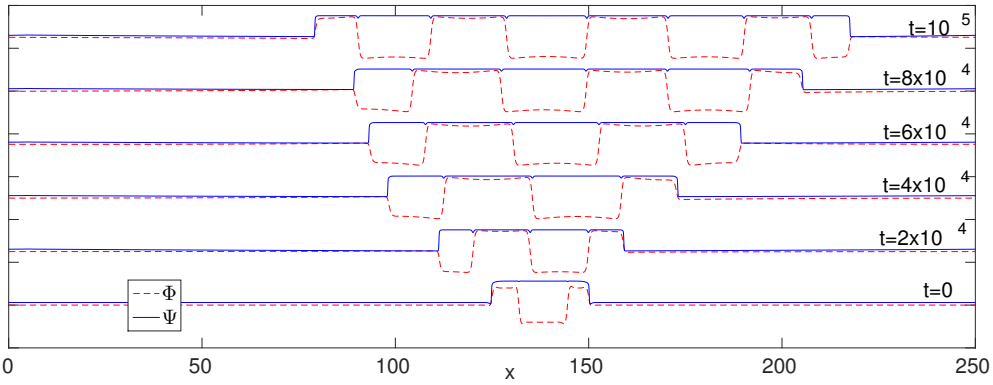

FIGURE 8. For large enough μ_ψ, there are no equilibria and the layered structure grows.

be minimized by having the polymer spread to infinity so that its concentration goes to zero. Notice that, for fixed chemical potential μ_Ψ, the effective multilayer volume

$$M_N \equiv \int_{x_0}^{x_N} \Psi(x)dx$$

exhibits a *quantization* phenomenon, since only a discrete set of values of M_N are allowed.

5.2. **Self-replication phenomenon.** In addition to describing multilayers of varying width, the parameter μ_Ψ also provides a threshold for dynamic behavior. For large enough μ_Ψ, theorem 1 does not hold. Numerical evidence suggests that this is not just an artifact of the analysis, but an indication of a bifurcation which produces qualitatively different behavior. Figure (8) shows the evolution of a bilayer initial condition when μ_Ψ is made sufficiently large. Pattern propagation ensues because the creation of new polymer subdomains is preferred over the supercritical mixture of solvent and polymer in the far field. This phenomenon is analogous to pattern self-replication which has been observed in many different systems [25, 26].

5.3. **Outlook.** Density functional models like (2) have been frequently utilized to study bulk and localized pattern formation in heterogeneous polymer systems. Numerical evidence [3–6] suggests that localized, layered structures should be widely observed in polymer systems exhibiting both microscopic and macroscopic phase separation. This paper provides a rigorous understanding of why this is the case, by showing that multilayered equilibria are, in a particular sense, energy minimizers.

Other limiting cases of the diffuse interface model are currently under investigation. These include a treatment where macroscopic segregation between polymer and solvent is a weaker, rather than stronger, effect. In addition, a dual scaling limit for α and Ψ_∞ results in a linearized version of equation (F1') which forms a tractable basis for the study of multidimensional stability.

We expect that multilayered structures are possible in higher dimensional settings also. In that case, various morphologies, such as spheres, tubes, and networks, might be expected. In addition, there are likely a variety of instabilities and dynamic behaviors worthy of theoretical investigation.

Appendix: common tangent relations and diffuse interfaces

Suppose that $W(\phi)$ is a smooth potential and has two local minima. Consider the constrained minimization problem

$$\min_{\phi\in Q}\int_0^L W(\phi)dx, \quad \int_0^L \phi\, dx = M,$$

where Q is the set of piecewise constant functions

$$\phi(x) = \begin{cases}\phi_1 & 0 < x < x_0\\ \phi_2 & x_0 < x < L.\end{cases}$$

Here L is the fixed domain size (which is arbitrary here) and $x_0 \in (0, L)$. Letting μ be the Lagrange multiplier, it is straightforward to check that the minimizer satisfies

$$W'(\phi_1) = \mu = W'(\phi_2), \quad \mu(\phi_2 - \phi_1) = W(\phi_2) - W(\phi_1). \tag{95}$$

This system of algebraic equations has a simple graphical solution, given by letting μ be the slope and $\phi_{1,2}$ the intersection points of a line doubly tangent to the graph of $W(\phi)$ (e.g. figure 3).

Consider now a diffuse interface described by the smooth profile $\phi(x)$, solving

$$-\phi_{xx} + W'(\phi) = \mu, \quad \phi(-\infty) = \phi_1, \quad \phi(+\infty) = \phi_2. \tag{96}$$

The first relation in (95) holds immediately by taking the limits as $x \to \pm\infty$. The second relation in (95) arises from the first integral of (96).

Acknowledgments

This work was supported by NSF award DMS-1514689.

References

[1] Karen I Winey, Edwin L Thomas, and Lewis J Fetters. Isothermal morphology diagrams for binary blends of diblock copolymer and homopolymer. *Macromolecules*, 25(10):2645–2650, 1992.
[2] Takeji Hashimoto, Satoshi Koizumi, and Hirokazu Hasegawa. Ordered structure in blends of block copolymers. 2. self-assembly for immiscible lamella-forming copolymers. *Macromolecules*, 27(6):1562–1570, 1994.
[3] Takao Ohta and Aya Ito. Dynamics of phase separation in copolymer-homopolymer mixtures. *Physical Review E*, 52(5):5250, 1995.
[4] Aya Ito. Domain patterns in copolymer-homopolymer mixtures. *Physical Review E*, 58(5):6158, 1998.
[5] T. Uneyama and M. Doi. Calculation of the micellar structure of polymer surfactant on the basis of the density functional theory. *Macromolecules*, 38(13):5817–5825, 2005.
[6] Takashi Uneyama. Density functional simulation of spontaneous formation of vesicle in block copolymer solutions. *The Journal of chemical physics*, 126(11):114902–114902, 2007.
[7] L. Leibler. Theory of microphase separation in block copolymers. *Macromolecules*, 13:1602–1617, 1980.
[8] T. Ohta and K. Kawasaki. Equilibrium morphology of block coploymer melts. *Macromolecules*, 19:2621–2632, 1986.
[9] T. Ohta and K. Kawasaki. Comment on the free energy functional of block copolymer melts in the strong segregation limit. *Macromolecules*, 23:2413–2414, 1990.
[10] J. W. Cahn and J. E. Hilliard. Free energy of a nonuniform system I. Interfacial free energy. *J. Chem. Phys.*, 28:258–267, 1957.
[11] Rustum Choksi and Xiaofeng Ren. Diblock copolymer/homopolymer blends: derivation of a density functional theory. *Phys. D*, 203(1-2):100–119, 2005.
[12] Yves van Gennip and Mark A. Peletier. Copolymer-homopoymer blends: global energy minimisation and global energy bounds. *Calc. Variations*, 33:75–111, 2008.
[13] Adam Blanazs, Steven P Armes, and Anthony J Ryan. Self-assembled block copolymer aggregates: From micelles to vesicles and their biological applications. *Macromolecular rapid communications*, 30(4-5):267–277, 2009.

[14] Yiyong Mai and Adi Eisenberg. Self-assembly of block copolymers. *Chemical Society Reviews*, 41(18):5969–5985, 2012.
[15] Qiang Du, Chun Liu, and Xiaoqiang Wang. A phase field approach in the numerical study of the elastic bending energy for vesicle membranes. *Journal of Computational Physics*, 198(2):450–468, 2004.
[16] M. A. Peletier and M. Röger. Partial Localization, Lipid Bilayers, and the Elastica Functional. *Archive for Rational Mechanics and Analysis*, 193:475–537, September 2009.
[17] Phil L Wilson, S Takagi, and H Huang. *The lipid bilayer at the mesoscale: a physical continuum model*. Springer, 2010.
[18] N. Gavish, G. Hayrapetyan, K. Promislow, and L. Yang. Curvature driven flow of bi-layer interfaces. *Physica D Nonlinear Phenomena*, 240:675–693, March 2011.
[19] Paul C. Fife and Danielle Hilhorst. The Nishiura-Ohnishi free boundary problem in the 1D case. *SIAM J. Math. Anal.*, 33(3):589–606 (electronic), 2001.
[20] T Ohta and M Nonomura. Elastic property of bilayer membrane in copolymer-homopolymer mixtures. *The European Physical Journal B-Condensed Matter and Complex Systems*, 2(1):57–68, 1998.
[21] Y. Nishiura and I. Ohnishi. Some mathematical aspects of the micro-phase separation of diblock copolymers. *Physica D*, 84:31–39, 1995.
[22] Xiaofeng Ren and Juncheng Wei. On the multiplicity of solutions of two nonlocal variational problems. *SIAM Journal on Mathematical Analysis*, 31(4):909–924, 2000.
[23] R. L. Pego. Front migration in the nonlinear Cahn-Hilliard equation. *Proc. R. Soc. Lond. A*, 422:261–278, 1989.
[24] Paul C Fife. *Dynamics of internal layers and diffusive interfaces*, volume 53. SIAM, 1988.
[25] Y. Nishiura and D. Ueyama. A skeleton structure of self-replicating dynamics. *Physica D Nonlinear Phenomena*, 130:73–104, June 1999.
[26] Karl B. Glasner. Spatially localized structures in diblock copolymer mixtures. *SIAM Journal on Applied Mathematics*, 70(6):2045–2074, 2010.

Karl Glasner, Department of Mathematics, University of Arizona
E-mail address: kglasner@math.arizona.edu